CHAPTER 5

TEMPERATURE AND FLOW TRANSDUCERS

Robert J. Moffat
Department of Mechanical Engineering
Stanford University
Stanford, California

1 INTRODUCTION **132**

2 THERMOCOUPLES **132**
2.1 Types and Ranges 132
2.2 Peripheral Equipment 133
2.3 Thermoelectric Theory 135
2.4 Graphical Analysis of Circuits 137
2.5 Zone-Box Circuits 138
2.6 Laws of Thermoelectricity 139
2.7 Switches, Connectors, Zone Boxes, and Reference Baths 142
2.8 Obtaining High Accuracy with Thermocouples 144
2.9 Service-Induced Inhomogeneity Errors 144
2.10 Thermoelectric Materials Connected in Parallel 147
2.11 Spurious emf due to Corrosion and Strain 148
2.12 Self-Validating Thermocouples 149
2.13 Thermocouple Probe Designs for Gas Temperature Measurements 150
2.14 Thermocouple Installations for Surface Temperature Measurement 151

3 RESISTANCE TEMPERATURE DETECTORS **152**
3.1 Types and Ranges 152
3.2 Physical Characteristics of Typical Probes 152
3.3 Electrical Characteristics of Typical Probes 153
3.4 Thermal Characteristics of Typical Probes 153
3.5 Measuring Circuits 155
3.6 The Standard Relationships for Temperature versus Resistance 157
3.7 Interpreting Temperature from Resistance: Common Practice 158

4 THERMISTORS **161**
4.1 Types and Ranges 161
4.2 Physical Characteristics of Typical Probes 161
4.3 Electrical Characteristics of Typical Probes 163
4.4 Thermal Characteristics of Typical Probes 163
4.5 Measuring Circuits and Peripheral Equipment 165
4.6 Determining Temperature from Resistance 166

5 OPTICAL METHODS **167**

6 ELECTRON NOISE THERMOMETERS **171**

7 ACOUSTIC VELOCITY PROBES **172**

8 TEMPERATURE-SENSITIVE COATINGS **173**

9 FLOW RATE **174**
9.1 Nomenclature 174
9.2 Basic Principles Used in Flow Measurement 175
9.3 Orifice, Nozzle, and Venturi Meters 176
9.4 Variable-Area Meters 177
9.5 Laminar Flowmeters 179
9.6 Instability Meters 180
9.7 Ultrasonic Flowmeters 181

REFERENCES **185**

Copyrighted Material

Reprinted from *Instrumentation and Control,* Wiley, New York, 1990, by permission of the publisher.

Copyright © 2006 John Wiley & Sons Retrieved from: www.knovel.com

1 INTRODUCTION

There are hundreds of different transducers for temperature and flow measurements. The most common types will be discussed in this chapter; some others will be mentioned only briefly.

In flow measurements, only closed-channel flow measurement techniques are considered here, and only for ''clean'' fluids. Slurries and liquids carrying large objects are not treated.

In temperature measurements, current interests range from cryogenics (a few kelvins) to plasmas (upward of 10,000 K). Most applications, however, are in the range from room temperature to 2000 K, and that is where the bulk of this chapter will be concentrated.

The accuracy of a temperature or flow measurement depends not only on the sensor characteristics but also on the interaction between the sensor and the system being instrumented. There are two primary classes of interactions: *system disturbance errors* (i.e., changes in the behavior of the system caused by the presence of the sensor) and *system/sensor interactions* (the sensor responding to more than one parameter of the system).

High-temperature measurements are subject to installation errors caused by heat transfer between the system and the transducer. The term *error* is defined as the difference between the observed value and the true value of the intended measurand. The output of a temperature sensor describes its own temperature, the *achieved temperature,* but the objective is usually to measure the temperature at a particular point in the solid, liquid, or gas into which the sensor is installed—the *available temperature.* There is often a significant difference between the available value and the achieved value because the sensor exchanges heat with its entire surroundings, not just with the immediate region around the sensor. It is not uncommon in high-temperature gas temperature measurements with unshielded sensors, for example, to have errors of several hundreds of degrees caused by radiation error, velocity error, or conduction error effects on the sensor. These errors cannot be accounted for by calibration of the sensor, nor can corrections be applied with any degree of certainty. The sensor must be protected by appropriate shielding. In most applications at high temperature, the installation errors are far larger than the calibration error of the sensor; hence, sensor accuracy does not mean the same as measurement accuracy.

Individual transducers are discussed in the following sections.

2 THERMOCOUPLES*

Thermocouples are the most commonly used electrical output transducers that measure temperature. They are inexpensive, small in size, and remarkably accurate when their peculiarities are understood.

2.1 Types and Ranges

Any pair of thermoelectrically dissimilar wires can be used as a thermocouple. The wires need only be joined together at one end (the measuring junction) and connected to a voltage-measuring instrument at the other end (the reference junction) to form a usable system. Whenever the measuring junction is at a different temperature than the reference junction, a voltage will be developed, which is related to the temperature difference between the two junctions. Several metallic materials are listed in Table 1 in order of thermoelectric polarity;

*Materials in this section is substantially derived from Ref. 2 with permission, except where otherwise referenced.

Copyright © 2006 John Wiley & Sons Retrieved from: www.knovel.com

Table 1 Thermoelectric Polarity Order of Metallic Materials

100°C	500°C	900°C
Antimony	Chromel	Chromel
Chromel	Nichrome	Nichrome
Iron	Copper	Silver
Nichrome	Silver	Gold
Copper	Gold	Iron
Silver	Iron	$Pt_{90}Rh_{10}$
$Pt_{90}Rh_{10}$	$Pt_{90}Rh_{10}$	Platinum
Platinum	Platinum	Cobalt
Palladium	Cobalt	Alumel
Cobalt	Palladium	Nickel
Alumel	Alumel	Palladium
Nickel	Nickel	Constantan
Constantan	Constantan	
Copel	Copel	
Bismuth		

Source: Reference 5.

each material in the listing is positive with respect to all beneath it. In an iron–palladium thermocouple, for example, the cold end of the iron wire will be positive with respect to the cold end of the palladium.

In some instances the operating temperatures of machinery elements have been measured using the machine structure as part of the thermoelectric circuit (cutting-tool tip temperatures, cam shaft/rocker arm contact temperatures, etc.). In such cases each material in the circuit must be calibrated, and all intermediate temperatures must be measured in order to interpret the signal.

The alloys usually used for thermoelectric temperature measurement are listed in Table 2. These have been developed over the years for the linearity, stability, and reproducibility of their electromotive force (emf)–temperature characteristics and for their high-temperature capability. Tables of thermocouple emf versus temperature [referenced to the international practical temperature scale of 1990 (IPTS9O)][1] are available as DOS files on a disk from the National Institute of Standards and Technology (NIST). The standardized letter-designated thermocouple pairs are treated: B, F, J, K, N, R, S, and T. This is the primary source for reliable thermocouple data.

The noble metal and refractory metal thermocouples are used generally with extension wires of substitute materials, which are cheaper and easier to handle (more ductile). The extension wires used are described in Table 3. Except for the substitute alloys, thermocouple extension wire is of the same nominal composition as thermocouple wire and differs from it mainly in the accuracy of its calibration and the type of insulation used. Extension wire is not calibrated as accurately as thermocouple-grade wire.

Thermocouple material can be purchased as individual bare wires, as flexible, insulated pairs of wires, or as mineral-insulated pairs swaged into stainless steel tubes for high-temperature service. Prices range from a few cents to several dollars per foot, depending on the wire and the insulation. There are many suppliers.

2.2 Peripheral Equipment

Any instrument capable of reading low-dc voltages (on the order of millivolts) with 5–10 μV resolution will suffice for temperature measurements; the accuracy depends upon the

Copyrighted Material

Copyright © 2006 John Wiley & Sons Retrieved from: www.knovel.com

Table 2 Common Alloys Used in Thermoelectric Temperature Measurement

Maximum Temperature		Allowable Atmosphere (Hot)	Material Names	Type ANSI[a]	Color Code	Average Output, mV/100°F	Accuracy[a]	
°F	°C						Std.	Spec.
5072	2800	Inert, H_2, vac.	Tungsten/tungsten–26% rhenium	—	—	0.86	—	—
5000	2760	Inert, H_2, vac.	Tungsten–5% rhenium/tungsten–26% rhenium	—	—	0.76	—	—
4000	2210	Inert, H_2, vac.	Tungsten-3% rhenium/tungsten-25% rhenium	—	—	0.74	—	—
3270	1800	Oxidizing[b]	Platinum–30% rhodium/platinum–6% rhodium	B	—	0.43	1/2%	1/4%
2900	1600	Oxidizing[b]	Platinum–13% rhodium/platinum	R	—	0.64	1/4%	1/4%
2800	1540	Oxidizing[b]	Platinum–10% rhodium/platinum	S	—	0.57	1/4%	1/4%
2372	1300	Oxidizing[b]	Platinel II (5355)/platinel II (7674)[c]	—	—	2.20	5/8%	—
2300	1260	Oxidizing	Chromel/Alumel,[d] Tophel/Nial,[e] Advance T1/T2,[f] Therm. Kanthal P/N[g]	K	Yellow-red	2.20	4°F,3/4%	2°F,3/8%
1800	980	Reducing	Chromel[a]/constantan	E	Purple-red	4.20	1/2%	3/8%
1600	875	Reducing	Iron/constantan	J	White-red	3.00	4°F,3/4%	2°F,3/8%
750	400	Reducing	Copper/constantan	T	Blue-red	2.50	3/4%	3/8%

Source: Reference 4.

[a] Per American National Standards Institute C96.1 standard

[b] Avoid contact with carbon, hydrogen, metallic vapors, silica, reducing atmosphere.

[c] © Englehard Corp.

[d] © Hoskins Mfg. Co.

[e] Wilber B. Driver Co.

[f] Driver–Harris Co.

[g] The Kanthal Corp.

Copyrighted Material
Copyright © 2006 John Wiley & Sons Retrieved from: www.knovel.com

Table 3 Extension Wires for Thermocouples

Thermocouple Material	Type	Extension Wire, Type[a]	Color[a] (+)	Color[a] (−)	Color[a] Overall
Tungsten/tungsten–26% rhenium	—	Alloys 200/226[b]	—	—	—
Tungsten–5% rhenium/tungsten–26% rhenium	—	Alloys (405/426)[b]	White	Red	Red[b]
Tungsten–3% rhenium/tungsten–25% rhenium	—	Alloys (203/225)[b]	White/yellow	White/red	Yellow/red
Platinum/platinum–rhodium	S,R	SX, SR	Black	Red	Green
Platinel II-5355/platinel II-7674	—	P2X[c]	Yellow	Red	Black[c]
Chromel/alumel, tophel/nial, Advance, Thermokanthal[d]	E	KK	Yellow	Red	Yellow
Chromel/constantan	K	EX	Purple	Red	Purple
Iron/constantan	J	JX	White	Red	Black
Copper/constantan	T	TX	Blue	Red	Blue

Source: Reference 4
[a] ANSI, except where noted otherwise.
[b] Designations affixed by Hoskins Mfg. Co.
[c] Englehardt Mfg. Co.
[d] Registered trademark names, see Table 2 for identification of ownership.

voltmeter. The signal from a thermocouple depends upon the difference in temperature between the two ends of the loop; hence, the accuracy of the temperature measurement depends upon the accuracy with which the *reference junction* temperature is known as well as the accuracy with which the electrical signal is measured.

Galvanometric measuring instruments can be used, but since they draw current, the voltage available at the terminals of the instrument depends not only on the voltage output of the thermocouple loop but also on the resistances of the instrument and the loop. Such instruments are normally marked to indicate the external resistance for which they have been calibrated. Potentiometric instruments, either manually or automatically balanced, draw no current when in balance and therefore can be used with thermocouple loops of any resistance without error. High-input-impedance voltmeters draw only minute currents and, except for very high resistance circuits, pose no problems. When in doubt, check the input impedance of the instrument against the circuit resistance.

The input stages of many instruments have one side grounded. Ground loops can result from using a grounded-junction thermocouple with such an instrument. If the ground potential where the thermocouple is attached is different from the potential where the instrument is grounded, then a current may flow through the thermocouple wire. The voltage drop in the wire due to the ground-loop current will mix with the thermoelectric signal and may cause an error.

2.3 Thermoelectric Theory

The emf–temperature calibrations of the more common materials are shown qualitatively in Fig. 1. The emf is the electromotive force *mv* that would be derived from thermocouples made of material *X* used with platinum when the cold end is at 0°C and the hot end is at *T*. Those elements commonly used as first names for thermocouple pairs [i.e., Chromel (–Alumel), iron (–constantan), copper (–constantan), etc.] have positive slopes in Fig. 1.

It can be shown from either the free-electron theory of metals or thermodynamic arguments alone that the output of a thermocouple can be rigorously described as the sum of

Copyrighted Material

Copyright © 2006 John Wiley & Sons Retrieved from: www.knovel.com

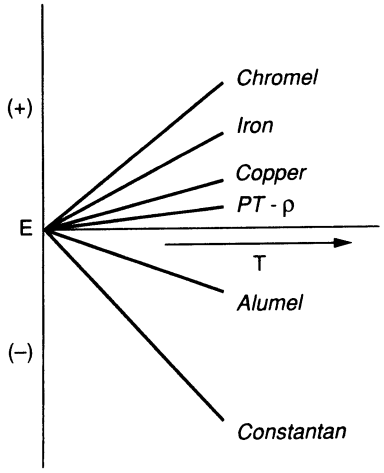


Figure 1 The emf vs. temperature calibrations for several materials. (Reproduced from Ref. 2, with permission.)

the contributions from each length of material in the circuit—the junctions are merely electrical connections between the wires. Formally,

$$E_{\text{net}} = \int_0^L \epsilon_1 \frac{dT}{dx}\, dx + \int_L^0 \epsilon_2 \frac{dT}{dx}\, dx \tag{1}$$

where ϵ = total thermoelectric power of material; equal to sum of Thomson coefficient and temperature derivative of Peltier coefficient
T = temperature
x = distance along the wire
L = length of the wire

When the wire is uniform in composition, so that ϵ is not a function of position,

$$E_{\text{net}} = \int_{T_0}^{T_L} \epsilon_1\, d\theta + \int_{T_L}^{T_0} \epsilon_2\, d\theta \tag{2}$$

Commercial wire is homogeneous within close limits, but used thermocouples may be far from uniform.

When only two wires are used in a circuit, it is customary to further simplify the problem. If both wires begin at one temperature (say T_0) and end at another (say T_L), the two integrals above can be collected:

$$E_{\text{net}} = \int_{T_0}^{T_L} (\epsilon_1 - \epsilon_2)\, d\theta \tag{3}$$

Three simplifications are built into this reduced equation:

1. ϵ is not a function of position (i.e., the wires are homogeneous).
2. There are only two wires.
3. Each wire begins at T_0 and ends at T_L.

These are the conditions for which the emf–temperature tables are intended. If any of the three conditions is not met, the tables cannot be used to interpret the output.

Copyrighted Material

Copyright © 2006 John Wiley & Sons Retrieved from: www.knovel.com

2.4 Graphical Analysis of Circuits

It is possible to graphically analyze a thermocouple circuit and describe its output in terms of the calibration of its wires. The simplest practical circuit consists of two wires joined together at one end and connected directly to a measuring instrument, as shown in Fig. 2. This is referred to as the *pattern circuit.* The pattern circuit is thermoelectrically ideal (providing that the materials of the instrument do not affect the reading) since it contains no switches, connectors, or lead wires. The output of this system can be analyzed graphically using the calibration data shown in Fig. 1. The method used here is described in detail by Moffat.[3]

The circuit in Fig. 2 requires frequent measurement of the temperature at the instrument terminals and is seldom used where accuracy of better than ± 2°F is required (chiefly because it is difficult to measure the temperatures of points 1 and 3 more accurately than ± 1°F).

A reference zone of controlled temperature eliminates the need for frequent measurements of the ambient temperature. The reference zone may be an ice point, a triple point, or an electrically controlled, high-temperature reference zone box. A circuit as in Fig. 3 assumes the reference temperature to be an ice-point bath.

The output of this circuit is the emf between points 1 and 5 (those connected to the instrument terminals). The ideal circuit would have had the output given by emf(2–4). The graphical construction shows that emf(2–4) is equal to emf(1–5) since the segments 1–2 and 4–5 each represent the same material (copper) over the same temperature interval ($T_{amb} - T_{ref}$), and the wires are connected so as to cancel these emfs. Thus, the actual circuit is thermoelectrically equivalent to the ideal circuit. Note that the copper lead wires (1–2 and 4–5) play no role in determining the output of the circuit, provided that (1) the calibrations

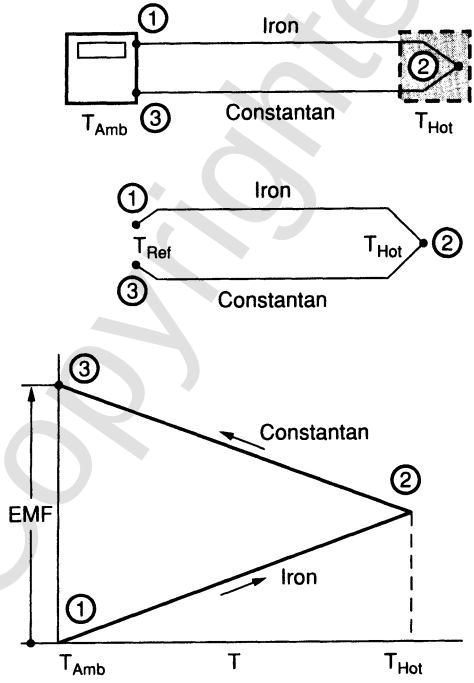


Figure 2 Temperature measurement using the ambient temperature as the reference. (Reproduced from Ref. 2, with permission.)

Copyrighted material

Copyright © 2006 John Wiley & Sons Retrieved from: www.knovel.com

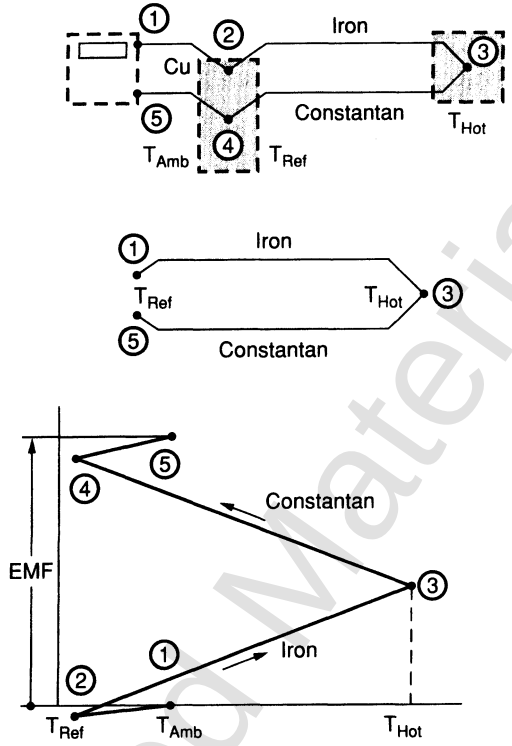


Figure 3 Temperature measurement using an icebath as the reference. (Reproduced from Ref. 2, with permission.)

of the two pieces of copper wire are the same and (2) the temperature intervals across the two copper wires are the same.

2.5 Zone-Box Circuits

When several thermocouples are used in a single test far from the measuring station, significant economies can sometimes be achieved by using a common zone box and substituting copper lead wires for much of the thermoelectric material. Such a circuit is shown in Fig. 4. The objective of the analysis is to determine the conditions under which the actual circuit is thermoelectrically equivalent to the pattern circuit.

The function of the zone box is to provide a region of uniform temperature within which connections can be made. The temperature of the zone box need not be constant, and it need not be known—it need only be uniform.

The circuit consists of a reference bath, a selector switch, a readout instrument, and a set of thermocouples extending from the zone box to their individual sensing points connected together with copper wires. Providing the selector switch and the lead wires introduce no spurious emf, the behavior of any one thermocouple for this circuit should be the same as that of the pattern circuit shown. In the E–T diagram, the copper lead wires are shown passing through the selector switch with no acknowledgment of its existence—the switch is assumed to have a uniform temperature at the ambient temperature.

Copyrighted Material

Copyright © 2006 John Wiley & Sons Retrieved from: www.knovel.com

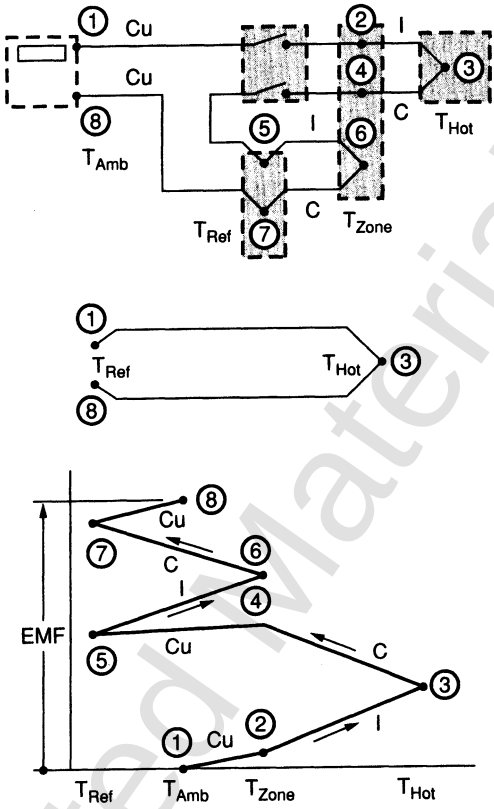


Figure 4 Multiple measurements using a zone box and selector switch. (Reproduced from Ref. 2, with permission.)

Commercially available zone-box and selector switch assemblies are sometimes made with the assumption that the junction 6 will be placed in the reference bath and points 5 and 7 in the zone box. This requires reversing the polarity of the reference junction (i.e., the wire between points 5 and 6 must then be constantan in this example, and the wire between 6 and 7 must then be iron).

If a wiring diagram is not available, a test for reference junction polarity should be made. With the system connected, at any arbitrary temperature, the instrument reading should go up if the temperature of the reference junction goes down, and conversely.

2.6 Laws of Thermoelectricity

Various authors have attempted to summarize the behavior of thermocouples through sets of laws ranging from three to six in number. One of the more detailed sets is given by Doebelin.[6] Each law can easily be proven by recourse to an emf–temperature sketch. The first three from Doebelin's list are used as examples:

1. The thermal emf of a thermocouple with junctions at T_{hot} and T_{ref} is totally unaffected by temperature elsewhere in the circuit if the two metals used are each homogeneous.

Copyrighted Material

Copyright © 2006 John Wiley & Sons Retrieved from: www.knovel.com

In Fig. 5, it is presumed that $T_{hot} < T_{candle}$. If the wire is uniform in calibration on both sides of the hot spot, the potential hysteresis loop closes and no net emf is generated because of the hot spot. The principal importance of this law is that it establishes the conditions under which a thermocouple is a point sensor. If and only if wires *A* and *B* are uniform in composition, the thermocouple output is determined only by the temperatures T_{ref} and T_{hot} and is independent of the temperature distribution along the wire.

2. If a third homogeneous metal *C* is inserted into either *A* or *B*, as long as the two new thermojunctions are at like temperature, the net emf of the circuit is unchanged irrespective of the temperature of *C* away from the junctions.

Figure 6 shows a third material inserted into the *A* leg and then heated locally. It is presumed that the temperatures at the two ends of *C* remain equal. If the material *C* is homogeneous, the emf induced by the excursion in temperature from point 2 to point 3 is canceled by that from point 3 to point 4, and no net signal is produced.

3. If metal *C* is inserted between *A* and *B* at one of the junctions, the temperature of *C* at any point away from the *AC* and *BC* junctions is immaterial. So long as the junctions *AC* and *BC* are both at the temperature T_1, the net emf is the same as if *C* were not there.

Figure 7 illustrates this case. An intermediate material, *C*, is inserted between *A* and *B* at the measuring junction. The diagram once more shows no change in the net emf if the inserted material is homogeneous and does not undergo a net temperature change.

The situation involving intermediate materials at the junction is of great practical importance because it addresses questions of manufacturing technique and how they affect thermocouple calibration. For example, the third material (*C*), used to connected the two materials *A* and *B*, might be the soft solder, silver solder, or braze material. The output of the thermocouple is independent of that third material, provided that the third material is homogeneous and begins and ends at the same temperature. In practice, these conditions are usually satisfied because the joining material is isothermal. If the third material is isothermal,

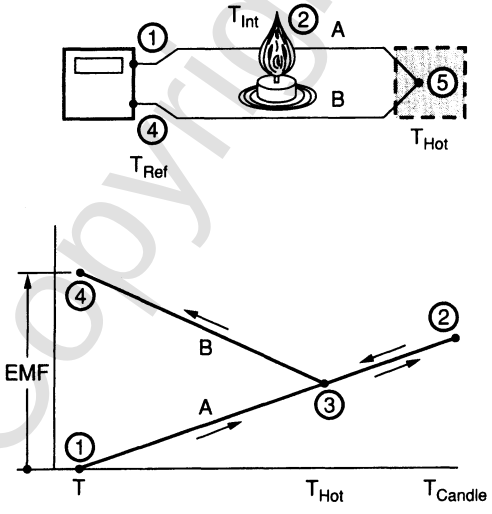


Figure 5 Illustration of the law of interior temperatures. (Reproduced from Ref. 2, with permission.)

Copyright © 2006 John Wiley & Sons Retrieved from: www.knovel.com

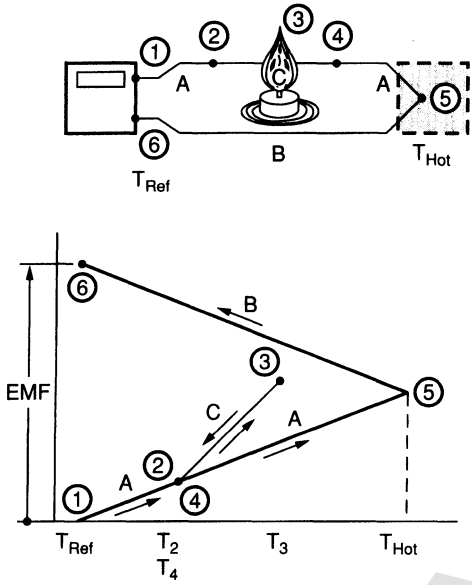


Figure 6 Illustration of the law of inserted materials. (Reproduced from Ref. 2, with permission.)

it makes no contribution to the output of the thermocouple. This proof should not be taken as a blanket license to connect thermocouple wires together without due care—some installations may result in temperature gradients near the junction, and those are sensitive to the presence of a joining material. However, a well-designed probe assures an isothermal zone around the junction, and those probes are insensitive to the material used to join the thermoelements together.

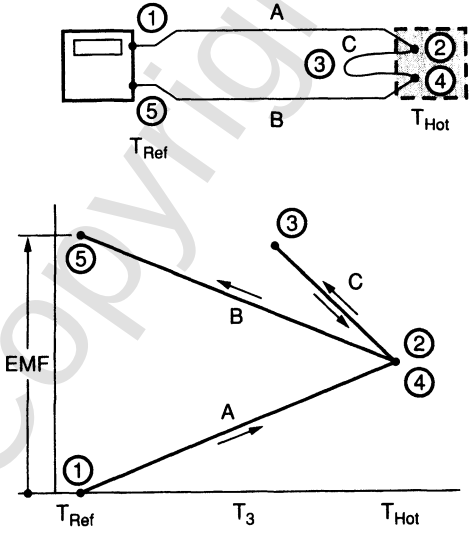


Figure 7 Illustration of the law of intermediate materials. (Reproduced from Ref. 2, with permission.)

Copyrighted Material

Copyright © 2006 John Wiley & Sons Retrieved from: www.knovel.com

2.7 Switches, Connectors, Zone Boxes, and Reference Baths

A thermocouple switch or connector must not produce emf that would contaminate the temperature signal. By their very nature, switches and connectors connect several materials together and are susceptible to generation of thermoelectric emf.

The principal defense against spurious emf is to ensure that the switch or connector is isothermal, not only on the whole but in detail. The mechanical energy dissipated as heat when the switch is moved appears first as a high-temperature spot on the oxide films of the two contacts. Substantial temperature gradients may persist for several milliseconds after a switch movement.

Connectors frequently are used to join a thermocouple to lead wires, often in a location near the test apparatus. Temperature gradients within connectors may generate spurious signals. It is important to insulate the outer shell and provide a good conduction path inside the connector.

Switches and connectors made of thermocouple grade alloys will minimize the troubles caused by poor thermal protection, but good thermal design is still necessary.

The errors that can be introduced by using a nonisothermal connector are illustrated in Fig. 8. An all-copper connector is presumed, with its connection points 2, 3, 5, and 6 as shown. Two cases are examined: one in which both the A and B wires enter at one temperature and leave at another ($T_2 = T_6$ and $T_3 = T_5$, but $T_2 \neq T_3$) and one in which the A wire

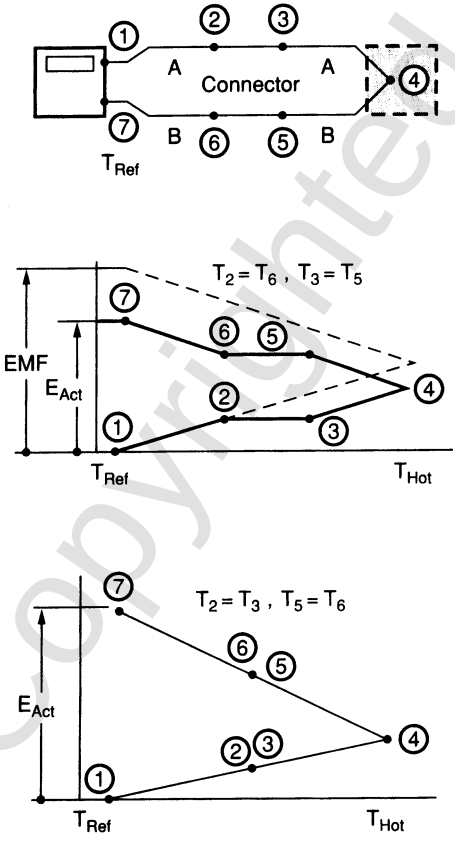


Figure 8 The effects of connectors. (Reproduced from Ref. 2, with permission.)

Copyrighted Material

Copyright © 2006 John Wiley & Sons Retrieved from: www.knovel.com

enters and leaves at one temperature while the *B* wire enters and leaves at some other temperature ($T_2 = T_3$ and $T_5 = T_6$, but $T_2 \neq T_5$). The *E–T* diagram shows the latter situation causes no error regardless of the type of material in the connector, since there is never a temperature gradient along the connector material. In the first case, the resultant signal is in error, having ''lost'' the entire amount of the temperature interval across the connector.

Reference baths which provide stable and uniform zones for termination of thermocouple systems are available. These generally consist of a heated or cooled zone box thermostatically controlled to remain at some specified temperature. Laboratory users may well use an ice bath or triple-point cell. For most engineering purposes, a bath made with ice and water sufficiently pure for human consumption will be within a few hundredths of a degree of 0°C if certain simple precautions are followed.

A Dewar flask or vacuum-insulated bottle of at least 0.5 liter capacity should be completely filled with ice crushed to particles about $\frac{1}{4}$ to $\frac{1}{2}$ cm in diameter. The flask is then flooded with water to fill the interstices between the ice particles. A glass tube resembling a small-diameter (0.5-cm), thin-walled (0.5-mm) test tube should be inserted 6 or 8 cm deep into the ice pack and supported there with a cork or float. A small amount (0.5 cm deep) of silicone oil should be placed in the bottom of the tube to improve the thermal contact between the junction and the ice-water mixture. The reference thermocouple junction is then inserted into the tube until it touches the bottom of the tube and is secured at the top of the tube with a gas-tight seal. The object of the seal is to prevent atmospheric moisture from condensing inside the tube and causing corrosion of the thermocouple.

The assembly is shown in Fig. 9, along with a proper connection diagram. Note that the relative polarity of the connection is different from that shown in Fig. 4. If a connection like Fig. 4 is desired, two glass tubes must be prepared, one each for the positive and negative

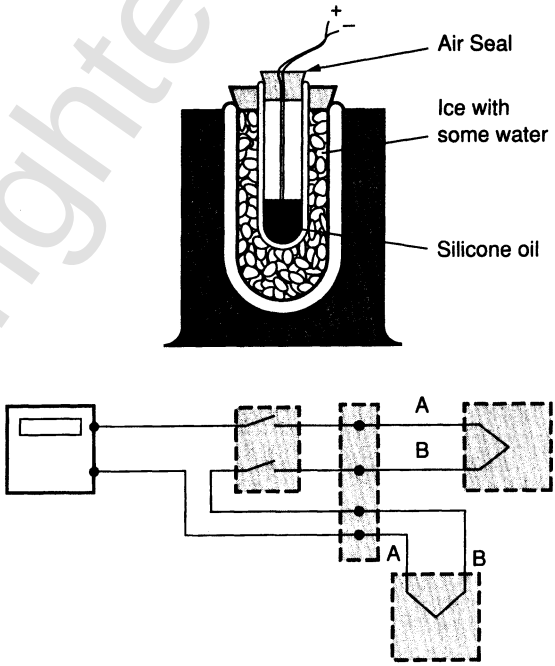


Figure 9 Construction of a reference ice bath. (Reproduced from Ref. 2, with permission.)

Copyrighted material

Copyright © 2006 John Wiley & Sons Retrieved from: www.knovel.com

elements. These tubes must be mounted farther apart than the size of the ice particles to assure adequate cooling. One thermoelement and one copper lead wire are put into each tube.

The principal requirement of the reference bath is that its temperature be known accurately. Any region of known temperature can serve as a reference bath.

Many instruments that provide their output in temperature units contain local reference regions and compensating circuits that augment the thermoelectric signal to account for the local reference temperature. Such instruments can be used only with the type of thermocouple for which they were intended, since the compensating network is specific to the calibration of the thermocouple being used.

2.8 Obtaining High Accuracy with Thermocouples

The temperature emf tolerances quoted for thermocouples account for two types of deviations from the expectation values: (1) batch-to-batch differences in average calibration and (2) point-to-point differences in local calibration along an individual thermocouple.

Calibration of individual thermocouples can account for the batch-to-batch differences but not the point-to-point variations along the wire.

For highest precision, three precautions should be taken:

1. Calibrate the individual thermocouples.
2. Minimize the working temperature difference (i.e., use a reference temperature near the working temperature and physically close by).
3. Install the thermocouple so the working temperature difference is stretched over as long a length of wire as possible.

2.9 Service-Induced Inhomogeneity Errors

When thermocouples are used in unfavorable environments or for very long times, the output voltage may drift with time.

There are many possible causes for this drift, among which are selective oxidation, which changes the composition of the alloy; diffusion of one or more of the components from the thermocouple alloys to the sheath of a mineral-insulated, metal-sheathed assembly; and local annealing of previous cold work. Most of these are ''high-temperature'' effects, occurring mainly between 500 and 1500°C, as described by Campari and Garribba[7] and Bentley.[8] Many of these effects are attributable to the complex composition of the thermoelectric alloys, according to Schuh and Frost,[9] who pointed out that the alloys were developed in the early and mid-1900s to generate an emf that was linearly proportional to temperature. This constraint, imposed by the widespread use of simple analog instruments, led to the ''tailoring'' of the emf characteristic by adding trace amounts of several constituents. With a complex composition, even small changes could significantly change the emf at a given temperature. Schuh and Frost pointed out that linearity is no longer an important issue since digital processing does not require linearity. They recommended increased attention to the use of high-temperature structural alloys as thermoelements, relying on ''smart'' instruments.

In the low-temperature domain, such as electronics cooling, one of the sources of inhomogeneity error is cold working of the thermocouple wire by bending. Type K is significantly vulnerable to this effect. The calibration of a type K pair can be lowered by 1% simply by bending the wires by hand. The error caused by this cold work depends on the severity of the cold work, the length of the damaged region of wire, and the temperature

Copyrighted Material

Copyright © 2006 John Wiley & Sons Retrieved from: www.knovel.com

difference across that length when the thermocouple is in service. The cold-worked region is often very short, which makes it difficult to detect.

A similar drop in calibration was reported by Bentley and Morgan[10] for PtRh versus Pt thermocouples in response to cold work introduced by handling. They reported a drop of about 0.4% in the cold-worked region. Annealing at 200°C did not entirely remove the drift in the PtRh leg. It is difficult to identify this problem by subsequent recalibration, since the region of partially degraded material may be placed in a uniform temperature zone during recalibration and hence play no part in generating the signal under calibration conditions. If a thermocouple is suspected of being inhomogeneous, it should be tested for homogeneity along its entire length. If the test shows that the wire is homogeneous, then no calibration is required, since the used portion of the wire is the same as the unused portion. If the wire is not homogeneous, no recalibration can be of value because it will be impossible to place the temperature gradient in the same location for calibration as it was for service. This situation is described in Figs. 10–12.

Assume that the thermocouple was exposed to the unfavorable environment only near the hot end, as shown in Fig. 10, and that both wires became less active as a result of the reaction. The output will drop, as shown. If this defective thermocouple were placed in a usual calibration facility, all of the affected material would be in the region of uniform temperature. The emf would be generated entirely by the material near the entrance of the furnace, which was never changed—the wires between points 1 and 2 and between 6 and 7 in Fig. 11. Under such conditions, a perfectly normal signal would be developed.

Figure 12 illustrates a test for homogeneity that can identify a defective thermocouple. To test a thermocouple for inhomogeneity, clamp the junction at a constant temperature and

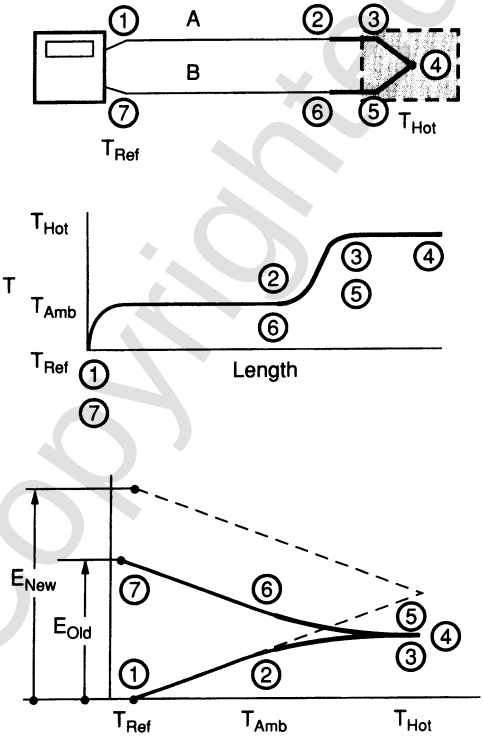


Figure 10 Temperature distribution along the thermocouple, in service, and the resulting output after deterioration of the wires. (Reproduced from Ref. 2, with permission.)

Copyrighted Material

Copyright © 2006 John Wiley & Sons Retrieved from: www.knovel.com

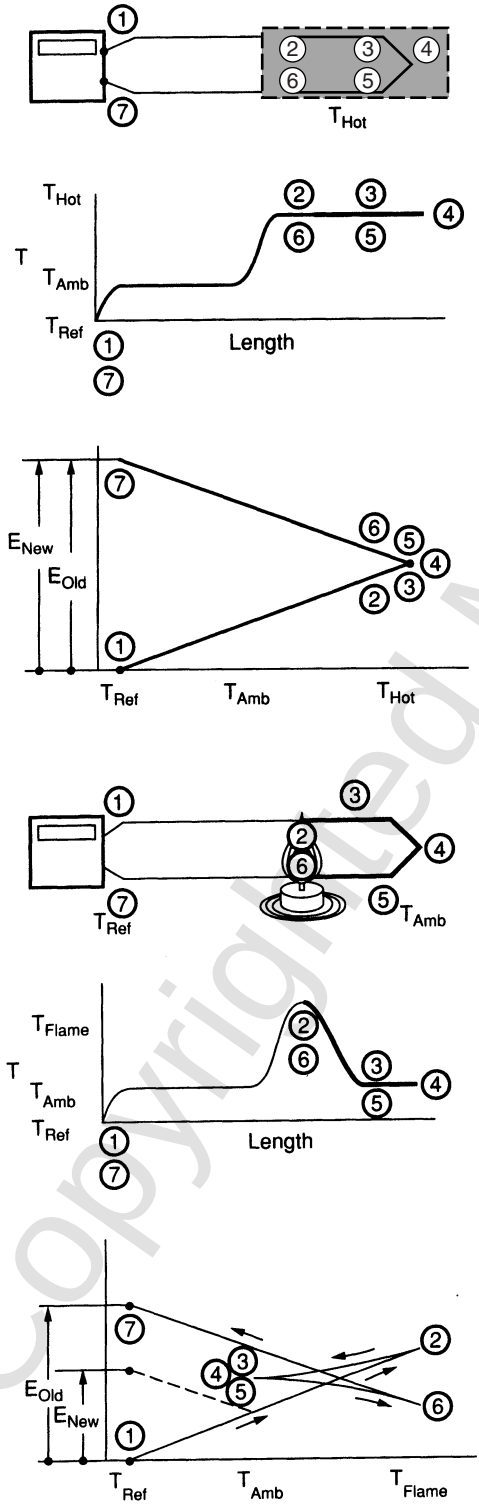


Figure 11 Temperature distribution along the thermocouple, during recalibration, and the resulting output. (Reproduced from Ref. 2, with permission.)

Figure 12 Homogeneity testing with a local hot spot and the resulting output. (Reproduced from Ref. 2, with permission.)

Copyrighted Material

Copyright © 2006 John Wiley & Sons Retrieved from: www.knovel.com

heat the wire in the suspected region. A homogeneous material will not produce any emf, as shown earlier in Fig. 5. An inhomogeneous material will have different calibrations on the upslope and downslope sides of the temperature excursion and will produce a net emf. This process is illustrated in Fig. 12.

The best technique for identifying a service-induced inhomogeneity is "side-by-side" running or comparison by replacement. Neither is very convenient, but on the other hand, there is no alternative. It is not within the present state of the art, regardless of how much effort is expended, to be able to interpret the readings from an inhomogeneous thermocouple in an arbitrary environment.

2.10 Thermoelectric Materials Connected in Parallel

Thermocouple materials are usually thought of as being connected in series with respect to the direction of the temperature gradient. There are situations, however, where two materials are in parallel electrical contact along their length. In such cases, the thermoelectric potential causes a distributed current to circulate in the materials. The net effect of such a configuration can be computed if the geometries and material properties are known.

There are three applications for which this effect is known to be of importance: (1) in the design of plated-junction thermopiles, (2) in attempts to precisely measure surface temperatures using thermocouples attached with solder, and (3) in the case of distributed failure of thermocouple insulation, usually at high temperatures.

The essential features of this parallel circuitry can be illustrated by discussion of the thermopile design and the shunted thermocouple situation.

Copper may be plated onto a constantan wire to form a cylindrical thermocouple pair in which the copper and constantan contact throughout their entire length. When the two ends of this plated material are held at different temperatures, an emf will be generated, which is a function of the relative electrical resistance of the two materials, as well as the usual thermoelectric parameters. The physical situation is shown in Fig. 13.

Gerashenko and Ionova[11] related the net emf to that of a conventional copper–constantan thermocouple by the following:

$$\frac{\text{EMF}}{\text{EMF}_{\text{std}}} = \frac{R_{\text{const}}}{R_{\text{const}} + R_{\text{copper}}} \tag{4}$$

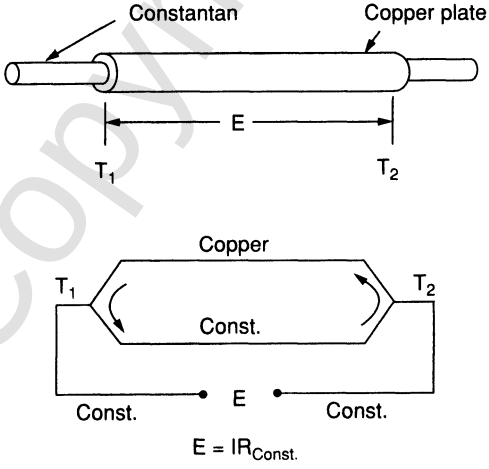


Figure 13 The plated junction thermopile element and its equivalent circuit. (Reproduced from Ref. 2, with permission.)

Copyright © 2006 John Wiley & Sons Retrieved from: www.knovel.com

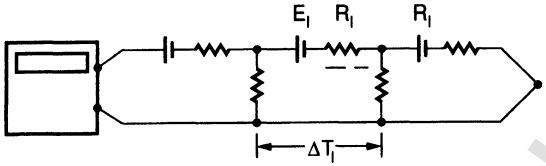


Figure 14 Electrical network model of the distributed shunt effect. (Reproduced from Ref. 2, with permission.)

where R is the electrical resistance for the component named in the length direction.

Thick copper platings will produce low resistance in the copper, and almost the entire output of the copper–constantan pair will be recovered.

There is another circumstance in which thermocouple elements become connected in parallel. When long thermocouples are used in hostile environments, there can be significant effects on the output due to partial shunting of the thermocouple by breakdown of the insulation between the wires. This effect was discussed in 1964 by Tallman,[12] who presented a model for numerical calculations to evaluate the output which is useful in explaining the behavior. The circuit shown in Fig. 14 describes the behavior when the insulators serve only as resistive connections between the wires (i.e., do not participate by generating emf). Only one node is shown in Fig. 14, although a real circuit would require many nodes for an accurate model:

$E_1 = \epsilon_{AB}(\Delta T_i)$
ϵ_{AB} = total thermoelectric power of AB pair
$R_i = R_A + R_B$ for ith interval
r_i = resistance between A and B wires in ith interval
ΔT_i = temperature difference across ith interval

This network can be solved by several techniques and seems to accurately model the physical behavior of the distributed shunt effect.

The problem of resistive shunting was revisited in 1999 by Gill and Nakos,[13] who were interested in measuring the temperatures of large pools of liquid fuel (diesel or jet fuel). Long runs of mineral-insulated thermocouple material were exposed to high temperatures (up to 1200°C). The resistance of the mineral-insulated thermocouple stock went down rapidly at high temperature, shunting the thermocouple signals. As a consequence, the apparent temperature was affected by the temperature in the shunt region as well as by the temperature at the measuring junction.

2.11 Spurious emf due to Corrosion and Strain

Thermocouples produce dc signals in response to temperature differences. They can also become sensitive to ac electrical noise and ground loops, all of which are tractable and can be handled as noise problems would be handled in any system.

There are two problems peculiar to the thermocouple that bear mention: galvanic emf generation and strain-induced emf.

Thermocouples necessarily involve pairs of dissimilar materials and hence are liable to galvanic emf generation in the presence of electrolytes. The iron–constantan pair is the most vigorous, being capable of generating a 250-mV signal when immersed in an electrolyte.

The galvanic emf generated between iron and constantan opposes the thermoelectric signal; that is, the voltage drop of the current through the measuring loop opposes the thermo-

Copyrighted Material

Copyright © 2006 John Wiley & Sons Retrieved from: www.knovel.com

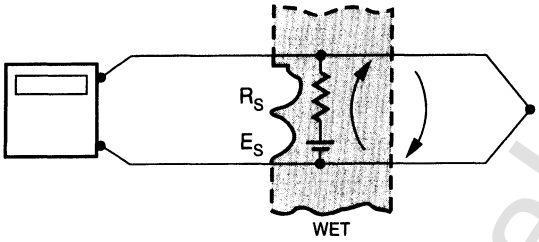


Figure 15 Electrical network model of the galvanic emf effect on a wet thermocouple. (Reproduced from Ref. 2, with permission.)

electric signal. The net effect, then, is that the thermocouple reads low. If the galvanic connection is near the junction, as it would be if certain soldering fluxes were not completely removed, the corrosive ''necking down'' of the iron wire increases the resistance to the galvanic current more and more as the wire is eaten away. This in turn means that the thermocouple readout circuit picks up a larger and larger fraction of the 250-mV galvanic signal. In bench tests of this mechanism,[14] it has been shown possible to have an iron–constantan thermocouple read negative (i.e., below the reference bath temperature).

Neither copper–constantan nor type K material shows significant galvanic effects.

The equivalent circuit is shown in Fig. 15. It is similar to the shunt problem, but the active emf source in the shunt dominates it.

The output of the system will be the thermoelectric emf corresponding to $T_{hot} - T_{ref}$ plus or minus the IR drop in the circulating current loop.

Typical values for E_{shunt} and R_{shunt} are 250 mV and 1 MΩ/cm of wetted length (24-gauge, duplex-fiberglass-insulated iron–constantan wires, wet with distilled water). The error induced by this signal depends on the resistance in the thermocouple loop and the location of the wet spot along the thermocouple. Wet iron–constantan thermocouples can produce large error signals.

Although type K materials do not display appreciable galvanic emf, they are strain sensitive (i.e., cold work causes a change in calibration), and during the act of straining, they generate appreciable emf. Temperatures measured on vibrating equipment may appear to fluctuate as a result of flexing of the thermocouple wires. Copper–constantan and iron–constantan are less active than type K, with copper–constantan least active. Spurious signals on the order of 50°C have been observed using type K materials on a vibrating apparatus (e.g., whole engine tests).

2.12 Self-Validating Thermocouples

Most thermocouple users blame the thermocouple for any ''bad'' data when, often, the fault lies elsewhere in the system—unrealistic expectations, poor installation of the sensor, and so on. As a consequence, there has been considerable interest in methods of ''validating'' a thermocouple's output while it is still in service.

One approach was to install the thermocouple junction in a capsule containing a metal or alloy whose melting temperature was known and was below the operating temperature of the thermocouple at steady state. On each ''fire-up,'' as the indicated temperature rose, the thermocouple trace would display a plateau at the melting point, thus confirming that the output was correct. A recent example of this approach was reported by Sachenko et al.,[15] who outfitted a Chromel–Alumel thermocouple with a capsule containing lead.

Copyrighted Material

Copyright © 2006 John Wiley & Sons Retrieved from: www.knovel.com

Industrial thermocouples are frequently installed in thermowells to isolate the sensor from the system. Often, the thermowell is partly filled with a fluid of high thermal conductivity to assure good thermal contact between the thermocouple and the system through the wall of the thermowell. An empty thermowell is one of the main causes of ''faulty thermocouple'' reports. This type of failure can be detected by an electrical heating test known as the loop current step response proposed by Hashemian[16] and more recently incorporated into the Oxford University SEVA (Self Evaluation) protocol by Yang and Clarke.[17] This procedure involves passing a current through the thermocouple to heat it above its operating temperature and recording the cooling curve obtained when the heating current is shut off. This procedure is executed periodically and the traces compared with a reference trace obtained when the thermocouple was first installed. Any loss of thermal contact between the thermocouple and its thermowell results in a change in the shape of the response curve in the first few seconds of the trace.

2.13 Thermocouple Probe Designs for Gas Temperature Measurements

Thermocouples respond to their total environment, including all heat transfer modes: radiation, conduction, and convection. Radiation and conduction tend to pull the thermocouple temperature away from the gas temperature toward the temperature of the radiating source or the conducting support structure. The thermocouple is ''connected'' to the gas temperature by convection through the heat transfer coefficient. The equilibrium temperature is that which results from an energy balance between these competing tendencies. In cases where chemical reactions may be catalyzed on the surface of the thermocouple, those mechanisms must also be considered. Any difference between the thermocouple temperature and the true gas temperature is considered an error. Three types of error are recognized: radiation error, conduction error, and velocity error. Each describes the difference between the true gas temperature and the indicated temperature due to one mechanism: radiant heat transfer, conductive heat transfer, or high-velocity viscous dissipation effects. The heat transfer characteristics of a thermocouple (which governs its response to its environment) is relatively well known and cannot be changed.

Designing a thermocouple probe for accurate gas temperature measurement consists in designing a protective envelope within which the thermocouple will be acceptably accurate, that is, within which the sum of all three errors will be acceptably small. No thermocouple probe can respond instantaneously to changes in gas temperature. Thermocouples (the junctions themselves, not including any surrounding probe structure) act as first-order systems in response to changes in temperature and compensation methods for first-order systems are well understood. The general procedure for design of gas temperature probes for steady-state accuracy and transient behavior has been described by Moffat.[18]

The following citations provide examples of these principles applied to probe design. Elmore and Watkins[19] developed an analog compensation system that used signals from two first-order thermocouples of different diameters to determine transient gas temperatures up to 1 kHz. The fundamental approach could be implemented using high-speed digital processing as well. Moffat[20] proposed a transient method for estimating the (steady) temperature of a very hot gas stream (above the melting temperature of the thermocouple). His method is based on briefly exposing the thermocouple to the gas stream and correcting the transient behavior using a first-order time constant. The appropriate value of the time constant is found by minimizing the variance in the corrected signal over the time interval of exposure of the thermocouple to the hot gas stream.

Copyrighted Material

Copyright © 2006 John Wiley & Sons Retrieved from: www.knovel.com

Radiation error plays an important role at high temperatures, especially in low-velocity situations. One approach to this problem is to use an aspirated probe to increase the gas velocity past the thermocouple junction, increasing the convective heat transfer coefficient and reducing radiation error. Suction pyrometer probes were investigated at the National Bureau of Standards during the 1950s for use in combustion chamber and afterburner studies, as reported by Lalos.[21] Norton et al.[22] adapted this method for use in a high-temperature glass furnace. Another approach is to use two probes with different (but predictable) error sensitivities and calculate the radiation error from the difference in the readings of the two probes. This approach has been used by Moffat[23] and Brohez et al.[24] The main problem with this approach is that the correction can be very large, and if the uncertainty in the raw data exceeds a few percent, then the correction becomes highly uncertain. The behavior of thermocouple probe designs in fire environments was investigated by Blevins and Pitts,[25] who modeled the behavior of bare thermocouples, single-shielded aspirated probes, and double-shielded aspirated probes under fire conditions. Pitts et al.,[26] of NIST's Building and Fire Research Laboratory, investigated the uncertainties in the corrected readings of bare and shielded, aspirated probes. Their results confirmed that the largest uncertainties were found when the corrections were largest.

Measurements in high-velocity gases suffer mainly from problems with the recovery factor of the probes. High-recovery-factor probes read close to stagnation temperature, but their recovery factor is sensitive to manufacturing tolerances and, therefore, is somewhat uncertain. Low-recovery-factor probes require larger corrections for the residual velocity error, but their simpler geometry can reduce the uncertainty in the final reading. Moffat[27] recommended a probe using a spherical tip (a ball bearing) whose recovery factor is very well known and repeatable, while Vasquez and Sanchez[28] describe the design of a system using a Kiel-type shield for a high-recovery probe. Both references dealt with applications requiring high accuracy in the measurement of small temperature differences—the temperature rise across a single stage of a compressor or turbine.

2.14 Thermocouple Installations for Surface Temperature Measurement

Two problems dominate the accuracy of surface temperature measurement with thermocouples: ensuring good contact between the sensor and the surface and avoiding disturbing the surface temperature by the presence of the thermocouple.

Keltner and Beck[29] analyzed the steady-state and transient errors of thermocouples attached to thick walls using the unsteady surface element method. Sobolik, Keltner, and Beck[30] dealt with thin plates, with special emphasis on the effect of the measurement errors on the interpretation of data from thin-foil heat flux gages.

Analysis of the surface measurement problem shows that thin-film thermocouples should be ideal sensors. Han and Wei[31] describe a method of making thin-film thermocouples on nonmetallic surfaces that yields excellent steady-state and transient measurement accuracy. They applied this technique to a Zirconia coating on an engine piston, but the thin-film concept would also be well suited to the electronics industry, which uses nonmetallic packaging and requires accurate measurement.

Not all thermocouple probes are attached to the surface—spring-loaded contact probes are often used for measurements in situations where no permanent attachment would be permitted. The error in such applications is dominated by the contact resistance. Osman, Eilers, and Beck[32] used an inverse conduction solution to develop a method for correcting transient measurements based on a steady-state calibration.

Copyright © 2006 John Wiley & Sons Retrieved from: www.knovel.com

3 RESISTANCE TEMPERATURE DETECTORS

The terms *resistance temperature detector* and *resistance thermometer* are used interchangeably to describe temperature sensors containing either a fine-wire or a thin-film metallic element, whose resistance increases with temperature. A small current (ac or dc) is passed through the element, and its resistance is measured. The temperature of the element is then deduced from the measured resistance using a calibration equation or a table.

3.1 Types and Ranges

Resistance temperature detectors can be designed for standards and calibration laboratories or for field service, although the probe designs are vastly different. Field service probes are generally encased in stainless steel protective tubes, with the wire or film elements bonded to sturdy support structures. They are made to handle considerable physical abuse. Laboratory standards probes are often enclosed in quartz tubes, with the resistance wire mounted in a strain-free manner on a delicate mandrel. High-precision temperature measurement requires that the element be strain free, so the electrical resistance is a function only of temperature, not of strain.

Resistance temperature detectors are well suited for single-point measurements in steady-state service at temperatures below 1000°C where long-time stability and traceable accuracy are required and where reasonably good heat transfer conditions exist between the probe and its environment.

These detectors are not recommended for use in still air or in low-conductivity environments unless the self-heating effect can be accounted for appropriately. They are not recommended for averaging service unless computer data acquisition and software averaging are contemplated. They are not recommended for transient service or dynamic temperature measurements unless specifically designed for such characteristics, since the usual probe is not amenable to simple time constant compensation.

Resistance temperature detector probes tend to be larger than some of the alternative sensors and to require more peripheral equipment (i.e., bridges and linearizers).

3.2 Physical Characteristics of Typical Probes

Probes intended for field service concentrate on ruggedness and repeatability. Their calibrations may not agree with the standard expectation values of laboratory-grade probes but should be repeatable. Drift tolerances on field service probes may be stated in terms of percent drift per 100 hours.

Probes for laboratory service are designed to ensure freedom from mechanical strain either due to fabrication or thermal expansion during service.

The bare sensing elements of resistance temperature detectors range in size from wafers $0.5 \times 1.0 \times 2.0$ mm, with pig-tail leads 0.25 mm in diameter and 2.5 cm in length, to wire-wrapped mandrels, again with pig-tail leads 4 mm in diameter and 2 cm in length. With protective tubes in place, typical probes range from 1.0 to 5.0 mm in diameter.

Some typical sensors and probes for field service are shown in Fig. 16. Stainless steel is used for the protection tubes on most such units. The sensing element can be either a wire wound on a mandrel or a thin film deposited on an insulating substrate. Wire resistance elements may also be bonded to their support structures and encapsulated in glass or ceramic, but strain-free, steel-jacketed probes are also available. Thin-film elements are usually formed directly on the substrate by sputtering or vapor deposition.

Some, but not all, laboratory-grade probes use quartz for the protection tubes. For highest accuracy and best long-term stability, the laboratory-grade probes use strain-free rigging

Copyright © 2006 John Wiley & Sons Retrieved from: www.knovel.com

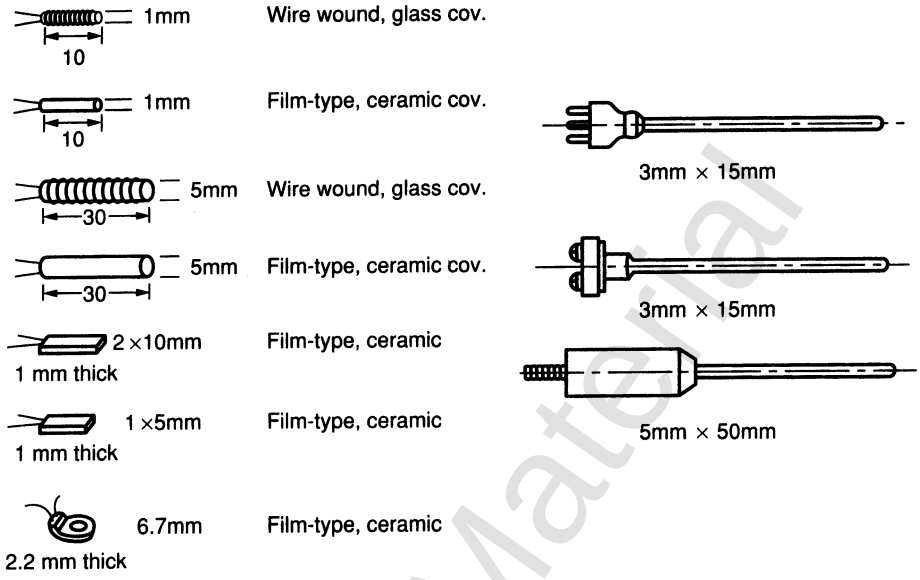


Figure 16 Physical characteristics of some sensors and probes.[33]

and a bifilar winding. This combination avoids the effects of mechanical strain on the resistance and also reduces pickup from electromagnetic or electrostatic fields. The windings are fragile, however, and the probes must be treated with great care. Figure 17 shows cutaway views of two laboratory-grade probes.

3.3 Electrical Characteristics of Typical Probes

Resistance–temperature detectors are available commercially with resistances from 20 to 2000 Ω, 100 Ω being common. Platinum, nickel, copper, and manganin have been used in commercial resistance thermometers.

Typically, the resistance of a platinum resistance thermometer will change by about 0.39%/°C. The resistance of a 100-Ω probe, according to the European calibration curve, would change by about 0.385 Ω/°C in the range 0–100°C. If the probe were in still air at 0°C and were being driven at a constant current of 3.16 mA (which would, on an average probe, produce a self-heating effect of about 0.25°C in still air), the voltage drop across the probe would be 316.304 mV, which would increase by 1.2166 mV for each degree Celsius increase in air temperature. By contrast, this compares to about 0.050 mV/°C for a typical base-metal thermocouple.

Twisted-pair lead wires are recommended. Care must be taken to avoid thermoelectric signal generation in resistance thermometer circuits using dc excitation (ac circuits convey the temperature information at carrier frequency, and they are not affected by thermoelectric signals).

3.4 Thermal Characteristics of Typical Probes

Interrogation of a resistance–temperature detector dissipates power in the element, which goes off as heat transfer to the surroundings. This self-heating causes the sensing element

Copyrighted Material

Copyright © 2006 John Wiley & Sons Retrieved from: www.knovel.com

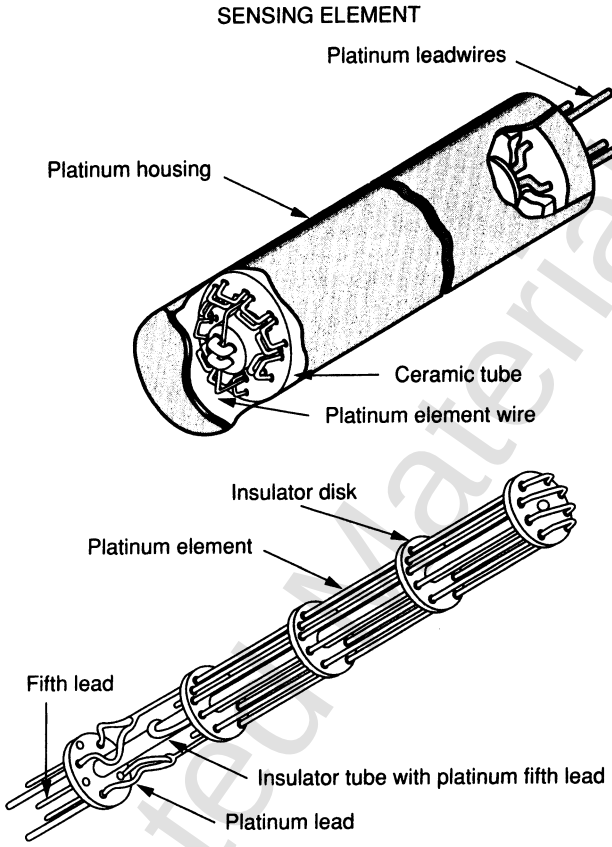


Figure 17 Cutaway views of two laboratory-grade probes.[34,35]

to stabilize at a temperature higher than its surroundings. The amount of self-heating depends on three factors: (1) the power dissipated in the element, (2) the probe's internal thermal resistance, and (3) the external thermal resistance between the surface of the probe and the surrounding material whose temperature is to be measured. The self-heating temperature rise is given by

$$T_{\text{sens}} - T_{\text{spec}} = W(R_{\text{int}} + R_{\text{ext}}) \tag{5}$$

A typical probe exposed to still air will display self-heating errors on the order of 0.1–1.0°C/mW (commercial probes of 1.5–5 mm in diameter). At 1 m/s air velocity, the self-heating error may only be 0.03–0.3°C, while in water (at 1 m/s velocity), the self-heating effect would be reduced by a factor of 4 or 5, depending on the relative importance of the internal and the external thermal resistances, compared to the values in moving air.

Self-heating error can be kept small by using probes with low internal thermal resistance, by locating the probes in regions of high fluid velocity (or placing the probes in tight-fitting holes in structures), or by operating at very low power dissipation. Pulse interrogation can also be used; it will reduce self-heating regardless of the internal and external resistances. The temperature rise of an element subjected to a pulse of current depends on the duration

Copyrighted Material

Copyright © 2006 John Wiley & Sons Retrieved from: www.knovel.com

of the pulse and the thermal capacitance of the sensor rather than on the resistances between the sensor and the specimen.

Resistance–temperature detectors (RTDs) are subject to all of the installation errors and environmental errors of any immersion sensor and, because of the detectors' larger size, are usually affected more than thermocouples or thermistors. Since RTDs are usually selected by investigators who wish to claim high accuracy for their data, the higher susceptibility to environmental error may be a significant disadvantage.

The internal structure of most RTDs is sufficiently complex that their thermal response is not *first order.* As a consequence, it is very difficult to interpret transients. The term *time constant,* which applies only to first-order systems, should not be applied to RTDs in general. If a *time constant* is quoted for a RTD, it may only mean "the time required for 63.2% completion of the response to a step change," and it may not imply the other important consequences of first-order response. Quoted values, from one probe supplier, of "time to 90% completion" range from 9 to 140 s for probes of 1.0–4.5 mm in diameter exposed to air at 1 m/s.

3.5 Measuring Circuits

Resistance–temperature detectors require a source of power and a means of measuring resistance or voltage.

Resistance can be deduced by voltage drop measurements across the resistor when the current is known or by comparison with a known resistor in a bridge circuit. Six circuits frequently used for *resistance thermometry* are shown in Fig. 18.

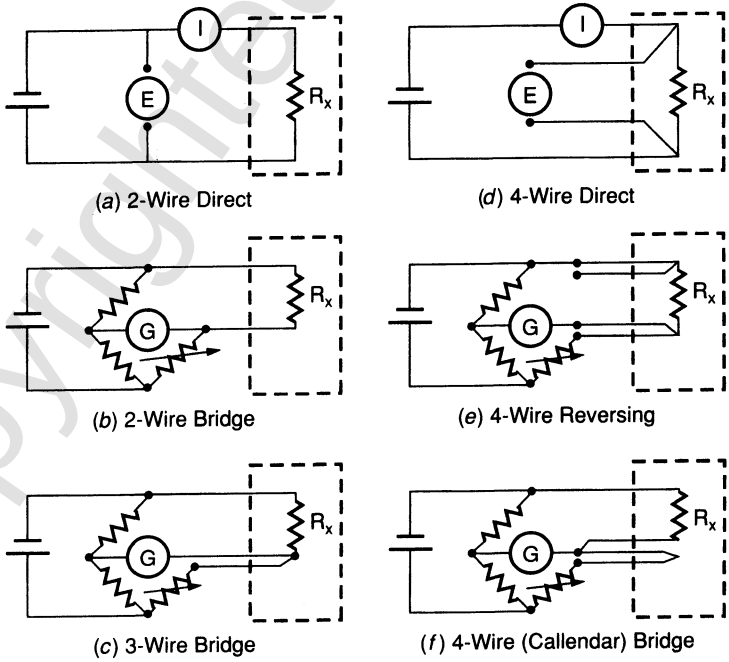


Figure 18 Six circuits for the measurement of resistance.

Copyrighted Material

Copyright © 2006 John Wiley & Sons Retrieved from: www.knovel.com

In the following paragraphs, these six circuits used for reading the resistance of the thermometer will be briefly discussed. The determination of probe temperature from probe resistance is discussed in a future section.

The two-wire, constant-current method is the simplest way to use a resistance thermometer. One simply provides it with a known current and measures the voltage drop across the probe and its lead wire (Fig. 18*a*). The resistance of the circuit is determined from Ohm's law in the cold and the hot condition, and the temperature is determined from the resistance ratio.

In this approach, the lead-wire resistance is ignored, which leads to underestimating the temperature change by approximately the ratio of the lead-wire resistance to the total circuit resistance:

$$\frac{R_{\mathrm{TOT},H}}{R_{\mathrm{TOT},C}} = 1 + \left(\frac{\Delta R_P}{R_{P,C} + R_L}\right) \tag{6}$$

Errors can be avoided by properly accounting for the lead-wire resistance, either by measuring it using a shorting plug to replace the probe or by calculating it from standard tabular data on wire resistance.

The two-wire bridge circuit (Fig. 18*b*) suffers from the same lead-wire error as the two-wire direct method but has one advantage: It can be used with an unstable power supply. The probe resistance can be measured in terms of the calibrated reference resistor, independent of the bridge voltage value.

The three-wire bridge circuit (Fig. 18*c*) compensates, to a considerable extent, for the effect of lead-wire resistance. The circuit uses a matched pair of lead wires to connect the bridge to the probe. One member of the pair is inserted into each of the two arms of the bridge, so changes in the lead-wire resistance affect both arms. For a bridge with equal resistances in both arms, this provides an approximate compensation for lead-wire resistance.

Many commercial probes are supplied with three-wire lead connection.

The most accurate technique for measuring the probe resistance is the four-wire direct method (Fig. 18*d*). Lewis[36] describes the advantages of the four-wire direct system in process industry measurements and points out that significant advantages in accuracy can be achieved at relatively low cost.

The probe is driven from a known source of constant current through one pair of leads, while the voltage drop across the sensing resistor is measured using the other pair. Since there is no current flow in the voltage-sensing leads, there is no error introduced by the lead-wire resistance. With current and voltage drop known, the resistance can be calculated directly using Ohm's law. Modern, regulated power supplies and high-impedance voltmeters make this an increasingly attractive option.

Two four-wire bridges are shown: the four-wire Callendar bridge and the reversing bridge. The Callendar bridge inserts equal lengths of lead wire in each of the two arms of the bridge, which provides good compensation for the effect of lead-wire resistance. The reversing bridge allows the operator to exchange lead wires, thus measuring the resistance in each arm with two different pairs of leads. The average of the two values is usually used as the best estimate, since the two measurements are equally believable.

Several manufacturers offer linearizing amplifiers as accessories for resistance thermometers. These devices produce signals that are linearly proportional to sensor temperature by correcting its nonlinear response.

The increasing use of computers in data interpretation has reduced the need for linearizing circuitry in laboratory and research work, but the commercial market still prefers linear systems for control and monitoring.

Copyright Material

Copyright © 2006 John Wiley & Sons Retrieved from: www.knovel.com

In some cases, the linearizing amplifier is provided as an integral part of the probe, which may also contain its own power supply. The output of such a probe is linearly proportional to the probe temperature.

3.6 The Standard Relationships for Temperature versus Resistance

Platinum resistance thermometers are sold in the United States under two different calibrations (U.S. and European) and are subject to tolerances, which can also be described by either of two standards.

The two calibrations differ in their expected values of α: the average temperature coefficient of resistivity ($\Omega/\Omega\cdot C$) over the interval 0–100°C. The European standard [Deutsches Institute für Normung (DIN) 43670] specifies α to be 0.003850 while the U.S. standard specifies 0.003925/°C. The IPTS-68 specified 0.003925 for probes acceptable as standards. The value of α increases with increasing purity, and values as high as 0.003927 have been observed, according to Norton.[37] Norton also mentions that thin films of platinum do not follow either of the two standard calibration curves just mentioned for bulk platinum but tend to approach the European standard value.

Table 4 illustrates the differences in resistance of U.S. and European calibrations.

From the user's standpoint, the important issue is, ''How much different are the temperatures deduced from a measured resistance?'' Figure 19 shows the temperature difference (European–U.S.) as a function of temperature level.

The equations proposed for data interpretation (i.e., the Callendar equation or the Callendar–Van Dusen equation) are attempts at fitting the tabular data—they are not the sources of the tables.

Just as there are different standards for the resistance–temperature relationship, so there are different standards for interchangeability among commercial probes. The hot resistance of a probe at a particular temperature depends on its cold resistance and its average value of α up to the operating temperature. Standards for interchangeability must acknowledge both sources of difference. Interchangeability is typically discussed in terms of ''percent of reading'' (in degree Celsius), with values from 0.1 to 0.6% being available in commercial probes for field service.

Table 4 Resistances of a Platinum Resistance Thermometer

Temperature, °C	U.S. Curve, $\alpha = 0.003925$	European Curve, $\alpha = 0.003850$
−200	17.14	18.53
−100	59.57	60.20
0	100.00	100.00
+100	139.16	138.50
+200	177.13	175.84
+300	213.93	212.03
+400	249.56	247.08
+500	284.02	280.93
+600	317.28	313.65

Source: Reference 37.

Copyrighted Material

Copyright © 2006 John Wiley & Sons Retrieved from: www.knovel.com

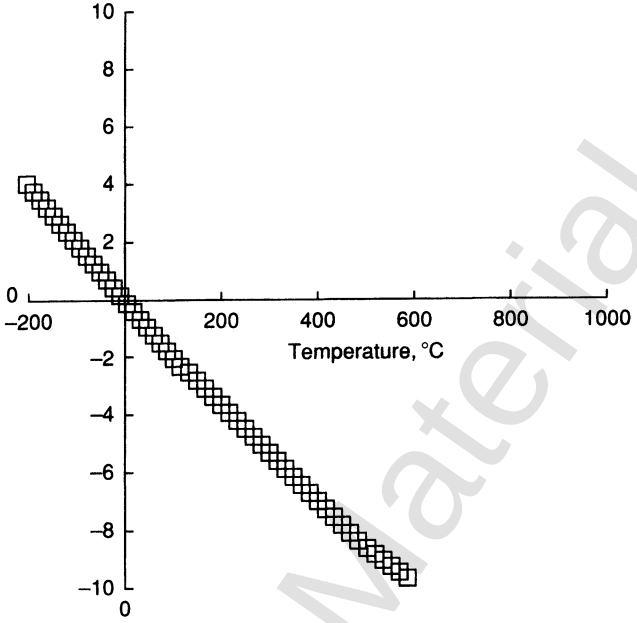


Figure 19 Comparison of the European and U.S. resistance curves.

The resistance–temperature characteristic of a probe may drift (i.e., change with time) while the probe is in service. Manufacturers of laboratory-grade probes will specify the expected drift rate, usually in terms of the expected temperature error over an interval of time. Two sample specifications are "0.01°C per 100 hours" for a low-resistance, high-temperature probe (0.22 Ω at 0°C, 1100°C maximum service temperature) and "0.01°C per year" for a moderate-resistance, moderate-temperature probe (25.5 Ω at 0°C, 250°C maximum service temperature). Drift of the resistance–temperature relationship appears related to changes in the grain structure of the platinum. Such changes take place more rapidly at high temperatures. Probes are annealed at high temperatures after fabrication in order to reduce the effects of manufacturing strains.

3.7 Interpreting Temperature from Resistance: Common Practice

The final step in determining the measured temperature is to interpret the probe resistance through a calibration relationship. There are several options depending on the accuracy required.

For rough work near the ambient, it is often good enough to simply take the nominal value of α as a constant and divide the observed change in resistance by the value of α to find the temperature change.

For work between 0 and 100°C, the *constant-*α method is quite accurate, since α was determined in this interval.

In general, manufacturers will provide resistance–temperature tables for their probes. These tables should be used only with the probes for which they were intended because they may not have any generality. Manufacturers' tables are slightly more accurate than the constant-α method.

Copyrighted Material

Copyright © 2006 John Wiley & Sons Retrieved from: www.knovel.com

For high-quality, laboratory-grade platinum resistance thermometers (used between 0 and 630°C), the Callendar equation describes the IPTS-68 temperature within ±0.045°C, according to Benedict.[38] The difference between IPTS-68 and the Callendar equation varies across the range of temperatures, as shown in Fig. 20.

The Callendar equation is

$$t = 100\left(\frac{R_t - R_0}{R_{100} - R_0}\right) + \delta\left(\frac{t}{100} - 1\right)\left(\frac{t}{100}\right) \tag{7}$$

where R_t = resistance at temperature t
R_0 = resistance at ice point
R_{100} = resistance at 100°C
δ = constant evaluated at zinc point (419.58)

As shown in Fig. 20, the tolerance of ±0.045°C represents an agreed-upon difference between the Callendar equation and the IPTS-68 equation.

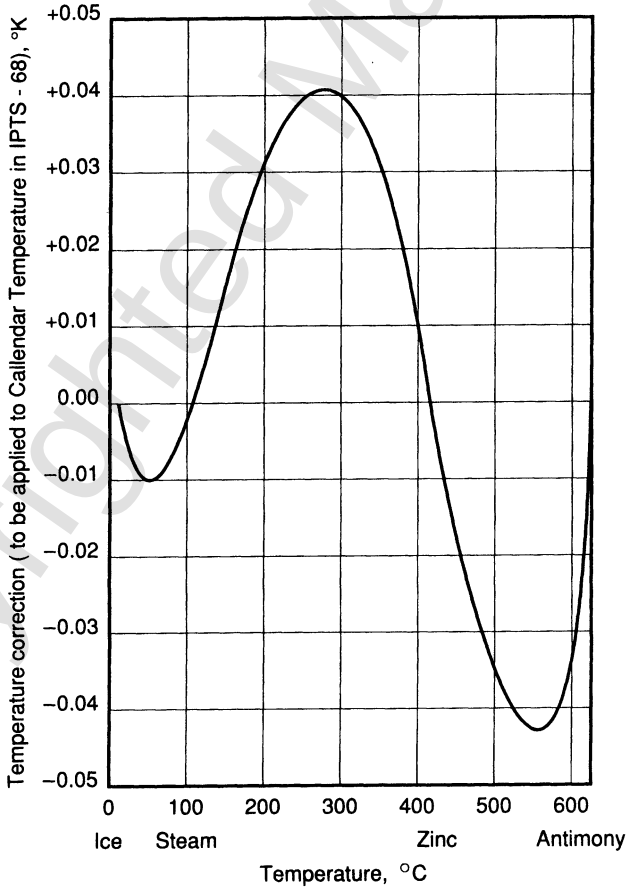


Figure 20 The difference between the Callendar equation and IPTS-68. (From Ref. 38, with permission.)

Copyrighted Material

Copyright © 2006 John Wiley & Sons Retrieved from: www.knovel.com

For most measurement purposes, the Callendar equation can be considered accurate within ±0.045°C over the range 0–630°C.

Below 0°C, temperature according to the Callendar equation deviates significantly from the IPTS-68 temperature. An additional term converts the Callendar equation into the Callendar–Van Dusen equation, which is much closer to the IPTS-68 temperature and is recommended for field service work between −190°C and 0°C.

The Callendar–Van Dusen equation is

$$t = 100\left(\frac{R_t - R_0}{R_{100} - R_0}\right) + \delta\left(\frac{t}{100} - 1\right)\left(\frac{t}{100}\right) + \beta\left(\frac{t}{100} - 1\right)\left(\frac{t}{100}\right)^3 \tag{8}$$

where R_t = resistance at temperature t
R_0 = resistance at ice point
R_{100} = resistance at 100°C
δ = constant determined at zinc point (419.58)

and

$$\beta = \begin{cases} 0 & t > 0 \\ \text{constant determined at oxygen point } (-182.962°\text{C}) & t < 0 \end{cases}$$

According to Benedict,[38] the disagreement between the Callendar–Van Dusen equation and IPTS-68 does not exceed ±0.03°C from −190 to 0°C. The difference varies, as shown in Fig. 21.

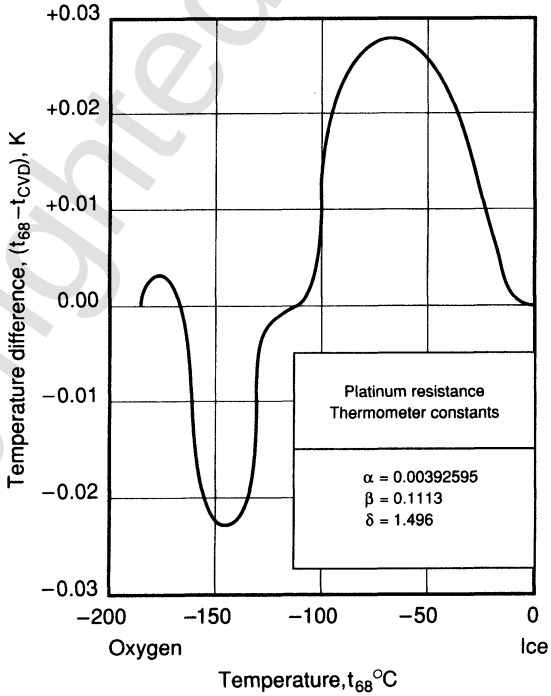


Figure 21 Difference between the Callendar–Van Dusen equation and IPTS-68. (From Ref. 38, with permission).

Copyrighted Material

Copyright © 2006 John Wiley & Sons Retrieved from: www.knovel.com

4 THERMISTORS

Thermistors are temperature-sensitive resistors whose resistance varies inversely with temperature. The resistance of a 5000-Ω thermistor temperature sensor may go down by 20 Ω for each degree Celsius increase in temperature (in the vicinity of the initial temperature). Driven by a 1.0-mA current source, this yields a signal of 200 mV/°C.

Thermistors are used frequently in systems where high sensitivity is required. It is not uncommon to find thermistor data logged to the nearest 0.001°C. This does not mean the data are accurate to 0.001°C, but the data are readable to that precision.

A thermistor probe is sensitive to the same environmental errors that afflict any immersion sensor: Its accuracy depends on the care with which it was designed for that particular environment.

4.1 Types and Ranges

Thermistor probes can be used between −183°C (the oxygen point) and +327°C (the lead point).[39] But most applications are between −80 and +150°C.[40] The sensitivity of a thermistor (i.e., the percent change in resistance per degree Celsius change in thermistor temperature) varies markedly with temperature, being highest at the lowest temperatures.

The long-time stability of thermistor probes is open to some question, although several months of accurate usage between calibrations seem attainable. The evidence on drift and its causes is not clear. It would be prudent, as with any temperature-measuring system, to make provision for periodic recertification of thermistor probes on a time scale established by experience within the system itself.

If accurate measurements are required, calibration facilities are needed, and this need poses some problems. Few instruments are capable of providing a transfer calibration for thermistors to their limit of readability, since few are that sensitive. Melting point baths and precision-grade resistance thermometry are needed to capitalize on the available precision.

Thermistors have strongly nonlinear output. Linearizing bridges are available, but these add to cost. Nonlinearity is not a significant issue when the data will be interpreted by computer.

4.2 Physical Characteristics of Typical Probes

Thermistor probes range in size from 0.25 mm spherical beads (glass covered) to 6-mm-diameter steel-jacketed cylinders. Lead wires are proportionately sized. Disks and pad-mounted sensors are available in a wide range of shapes, usually representing a custom design gone commercial. Aside from the unmounted spherical probes and the cylindrical probes, there is nothing standard about the probe shapes.

Figure 22 shows some representative shapes of commercially available probes.

For medical applications, thermistor probes are often encapsulated in sterilizable, flexible vinyl material. Such probes are frequently taped to a patient's skin and used as the control sensor for the temperature-regulating system.

The thermistor element itself is fabricated using the techniques of powder metallurgy. A mixture of metallic oxides is compressed into a disk and sintered. The mixture's composition, the sintering temperature, and the atmosphere in the furnace determine the resistance and the resistance–temperature coefficient of the thermistor. The faces of the disk are plated with silver, and the resistance of the thermistor is adjusted by removing material from the edges until the desired value has been obtained. The lead wires are attached, and the assembled thermistor is then potted in epoxy, rubber, or glass.

Copyright © 2006 John Wiley & Sons Retrieved from: www.knovel.com

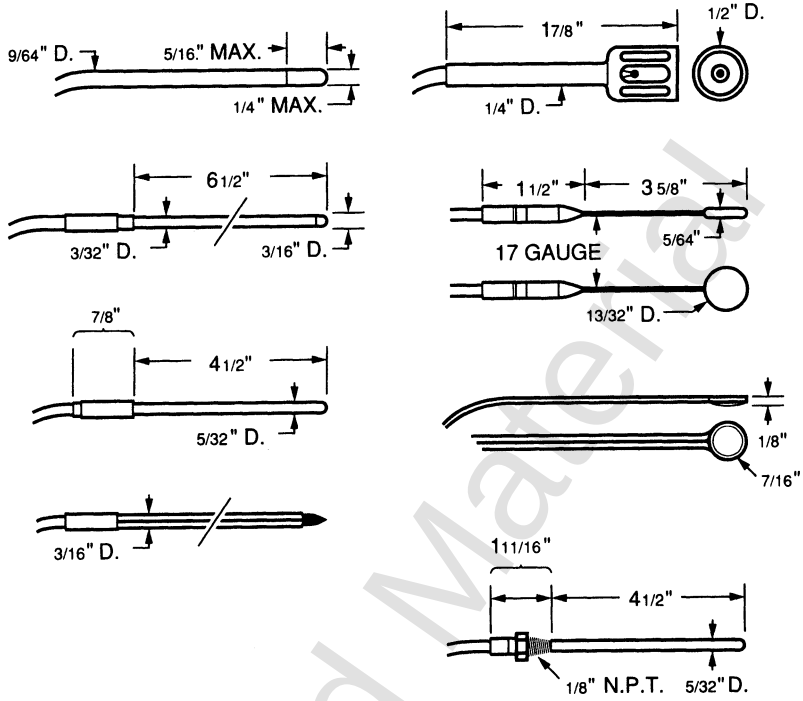


Figure 22 Representative thermistor probes for temperature measurement. (Courtesy of Omega Engineering, F4 of 1985 catalog.)

Resistance drift with time is a problem with some thermistor materials, especially at higher temperatures. Park[41] recommends the addition of SiO_2 to the mixture of oxides generally used for negative-coefficient thermistor material as a means of stabilizing the resistance–temperature characteristic.

The process is shown schematically in Fig. 23.

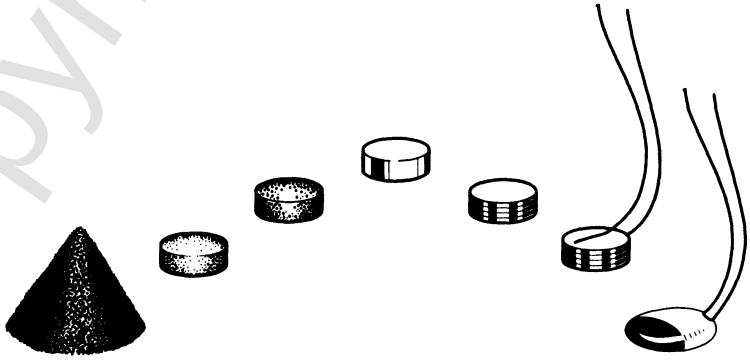


Figure 23 The thermistor manufacturing cycle.

Copyrighted Material

Copyright © 2006 John Wiley & Sons Retrieved from: www.knovel.com

High-temperature thermistors (1000°C) have been made from doped ceramic materials but with only moderate success.

4.3 Electrical Characteristics of Typical Probes

Thermistor probes vary in resistance from a few hundred ohms to megohms. Resistance is frequently quoted at 25°C with no power dissipation in the thermistor. The commercial range is from about 2000 to 30,000 Ω.

The resistance–temperature characteristic of a thermistor depends on the material of which it is made. Representative values of the sensitivity coefficient (percent change in resistance per degree Celsius) are given in Table 5.

To illustrate the range of resistances encountered in practice, Table 6 shows the resistance as a function of temperature for a typical probe whose resistance is 2252 Ω at 25°C.

Thermistor resistance data are frequently shown as logarithm of resistance ratio versus $1/T$. Such a presentation emphasizes the ''almost linearity'' of a single-term exponential description of the resistance–temperature characteristic. The data listed in Table 6 are shown in Fig. 24.

Proprietary probes are available that *linearize* thermistors by placing them in combination with other resistors to form a circuit whose overall resistance varies linearly with temperature over some range. These compound probes can be summed, differenced, and averaged like any linear sensor.

Modem manufacturing practices allow matched sets of thermistors to be made interchangeable within ±0.1°C.

4.4 Thermal Characteristics of Typical Probes

Thermistor probes are generally interrogated using a current of 1–10 μA, either ac or dc. With a probe resistance of 10 Ω, this results in power dissipation of 0.01 W that must be transferred from the probe into its surrounding material. At the first instant of application, this current has no significant effect on the measured resistance of the probe, but in steady state, it results in the probe running slightly above the temperature of the medium into which it is installed. This is referred to as the *self-heating* effect. Since thermistors are often used where very small changes in temperature are important, even small amounts of self-heating may be important.

Table 5 Variations of Thermistor Temperature Coefficient with Temperature

Temperature (°C)	Condition	%/°C
−183	Liquid oxygen	−61.8
−80	Dry ice	−13.4
−40	Frozen mercury	−9.2
0	Ice point	−6.7
25	Room temperature	−5.2
100	Boiling water	−3.6
327	Melting lead	−1.4

Source: Reference 39.

Copyrighted Material

Copyright © 2006 John Wiley & Sons Retrieved from: www.knovel.com

Table 6 Variation of Thermistor Resistance with Temperature

Temperature (°C)	Resistance (Ω)	Temperature (°C)	Resistance (Ω)
−80	1.66 M	0	7355.0
−40	75.79 K	25	2252.0
−30	39.86 K	100	152.8
−20	21.87 K	120	87.7
−10	12.46 K	150	41.9

Source: Reference 43.

The self-heating response is frequently discussed in terms of the *dissipation constant* of the probe, in milliwatts per degree Celsium. Dissipation constants can range from 0.005 mW/°C to several watts per degree Celsius and can be estimated with acceptable accuracy, given the geometry and thermal properties of the probe and its installation. The dissipation constant should not be used to correct a reading for the self-heating effect; the uncertainty in the correction is too high. If a calculation shows the self-heating effect to be significant, pulse interrogation should be used.

Dissipation constants for two representative probes are given in Table 7.

The self-heating effect must be considered in calibration as well as in use. Calibration baths frequently use stirred oil as the medium. Table 7 shows the self-heating effect in the oil bath to be very low compared to that in air at 5 m/s. A probe calibrated in an oil bath and used in air would be subject to different self-heating effects, and the user should be aware of that.

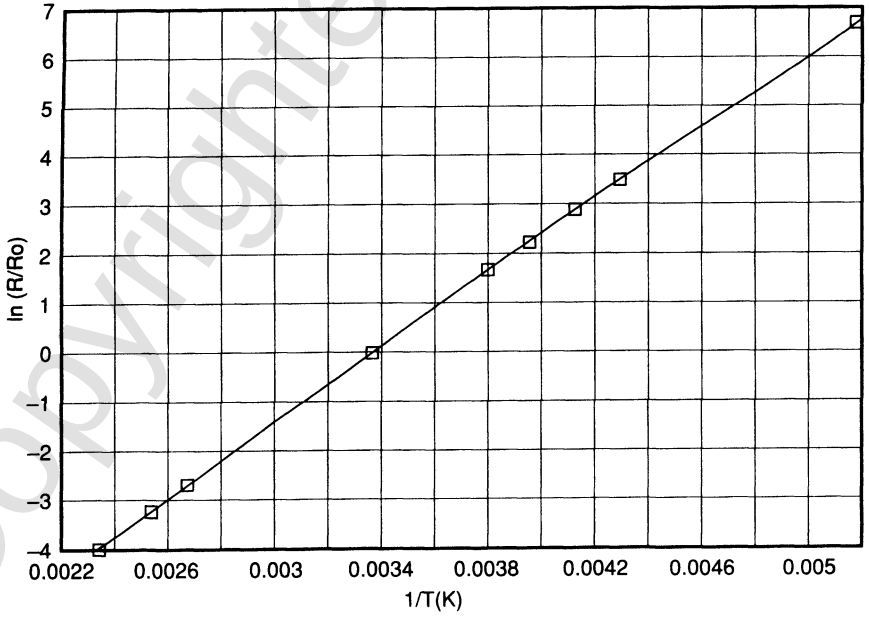


Figure 24 Resistance ratio of a typical thermistor as a function of $1/T$ (K).

Copyrighted Material

Copyright © 2006 John Wiley & Sons Retrieved from: www.knovel.com

Table 7 Representative Thermal Dissipation Constants for Two Different Thermistor Probe Designs

Environment	1.0-cm Disk	5.0-cm Glass Cylinder
Still air	8 (mW/°C)	1 (mW/°C)
Air at 5 m/s	35	—
Still oil	55	3.5
Still water	—	5
Oil at 1 m/s	250	—

Source: Reference 39.

The transient response of thermistors is more complex than that of thermocouples, and they are not as well suited to transient measurements. The difference arises from the thermal response of the thermistor material itself. Thermistor materials typically have lower thermal diffusivity than metals and hence do not equilibrate their internal temperatures as rapidly, all other factors being the same. Thus the highest frequency at which a thermistor will yield a first-order response is far lower than that for a thermocouple. During rapid changes, the temperature is not uniform inside the thermistor, and the average resistance no longer describes the average temperature. Since the thermistor resistance is not a linear function of temperature, the transient resistance cannot easily be converted to temperature.

Thermistor probes are susceptible to environmental errors (radiation, velocity, and conduction errors) as are all other immersion temperature sensors, and the same guidelines and design rules apply.

Thermistor sensors can be built into complex probe designs, as can any temperature sensor, and the structure of the probe will determine its steady-state and transient behavior. The thermistor has relatively low thermal conductivity and is frequently encapsulated in epoxy, glass, or vinyl, which also have low thermal conductivity. On this account, the transient response of a thermistor probe will be slower and more complex than that of a metallic sensor.

Tagawa et al.[42] analyzed the transient response of spherical and planar thermistors and showed that some configurations can be treated as first-order systems for slow changes in temperature, although they display second- or third-order characteristics at higher frequencies. They reported success using time constant compensation to reduce the compensated time constant by factors as large 50.

4.5 Measuring Circuits and Peripheral Equipment

Electrical resistance is easily measured within ordinary levels of accuracy by a number of techniques, and any method can be used with thermistors. The logarithmic variation of resistance with temperature means that over small ranges a constant percent error in resistance translates into a fixed error in temperature level. For example, with a thermistor whose sensitivity coefficient (see Table 5) is 5%/°C, a resistance measurement accurate to $\pm 0.1\%$ of reading will yield a temperature measurement accurate within ± 0.02°C everywhere in the range. Accuracy of this order can be achieved by two-wire and four-wire systems using off-the-shelf instruments and thermistors.

When thermistors are used to resolve very small differences in temperature (e.g., into the milliKelvin resolution range), special precautions must be taken to measure the resistance

Copyright © 2006 John Wiley & Sons Retrieved from: www.knovel.com

with the required accuracy. For the sensitivity mentioned above, 50 ppm corresponds to about 1 mK. Measurements in the 1–100-mK range are more typical of standards room practice than of field measurements, yet some applications require this precision.

4.6 Determining Temperature from Resistance

Experimental evidence shows that the resistance of a thermistor varies inversely and nearly exponentially with temperature. This suggests expressing the resistance–temperature relationship as a polynomial in $\ln(R)$:

$$\frac{1}{T} = A_0 + A_1 \ln(R) + A_2 \ln(R)^2 + A_3 \ln(R)^3 + \cdots + A_N \ln(R)^N \tag{9}$$

Note the R is dimensional in this equation; hence the values of the constants would depend on the units used for R.

A form retaining terms through the cubic, sufficiently accurate for small ranges in temperature, was used by Steinhart and Hart.[44] Their results indicated that the second-order terms had no effect, but later work has shown some advantage in retaining these terms. However, the Steinhart–Hart equation is still widely used:

$$\frac{1}{T} = A_0 + A_1 \ln(R) + A_3[\ln(R)]^3 \tag{10}$$

Arguments concerning the need for dimensional homogeneity led Bennet[45] to propose a dimensionless form which is independent of the units used:

$$\frac{1}{T} - \frac{1}{T_0} = A_1 \ln\left(\frac{R}{R_0}\right) + A_2 \ln\left(\frac{R}{R_0}\right)^2 + \cdots + A_N \ln\left(\frac{R}{R_0}\right)^N \tag{11}$$

Justification for this form can be seen in the near-linearity of Fig. 24.

This general form has given rise to several simplified forms. For a first approximation, only one term is needed:

$$R = R_0 \exp\left[A_1\left(\frac{1}{T_0} - \frac{1}{T}\right)\right] \tag{12}$$

This form reveals the exponential nature of the thermistor resistance response to changes in temperature.

Seren et al.[46] compared four different forms of the calibration equation for goodness of fit to a data set covering a range of 200 K, published by Bosson, Guttmann, and Simmons,[47] and accepted the data set as reliable. Their results are shown in Table 8. The following calculations were used to arrive at those results:

Table 8 Accuracy of Least-Squares Fits of Four Different Polynomial Expressions for Thermistor Calibration

Form of Equation for $1/T$	SRE	RMS Error	Mean Error
1. $A_0 + A_1 \ln(R)$	0.00601	1.999	0.1925
2. $A_0 + A_1 \ln(R) + A_2[\ln(R)]^2$	0.000428	0.1353	−0.0026
3. $A_0 + A_1 \ln(R) + A_2[\ln(R)]^2 + A_3[\ln(R)]^3$	0.000139	0.0392	0.00008
4. $A_0 + A_1 \ln(R) + A_3[\ln(R)]^3$	0.000138	0.0380	−0.00001

Source: Reference 47.

Copyrighted Material

Copyright © 2006 John Wiley & Sons Retrieved from: www.knovel.com

SRE = standard relative error, the root-mean-square of the relative errors at the test points:

$$\text{SRE} = \left[\sum_{i=1}^{n} \frac{(T_{c,i} - T_{0,i})^2 / T_{0,i}^2}{n} \right]^{1/2} \tag{13}$$

RMS error = root-mean-square error:

$$\text{RMS} = \left[\frac{1}{n} \sum_{i=1}^{n} (T_{c,i} - T_{0,i})^2 \right]^{1/2} \tag{14}$$

Mean error = algebraic mean error:

$$\text{Mean} = \frac{1}{n} \sum_{i=1}^{n} (T_{c,i} - T_{0,i}) \tag{15}$$

where T_c = calculated temperature (K) at measured resistance R_i
T_i = observed temperature at measured resistance R_i

The fourth form is the Steinhart–Hart equation. It seems, from this comparison, that there is little to choose from between the two cubic fits as far as goodness of fit is concerned, and since the Steinhart–Hart form requires only three constants, it would be preferred.

A calibration equation such as the Steinhart–Hart equation would be used with a commercial probe only when the highest accuracy is required. In most cases, the manufacturer's calibration is sufficiently accurate.

Thermistor probes are sold with resistance–temperature calibration tables accurate within ± 0.1 or 0.2 K, depending on the probe grade purchased. These tables are typically in 1-K increments. For computer interpretation, they should be fit to the Steinhart–Hart form and the coefficients determined for least error.

For the highest precision in measurement of temperature level, the purchased thermistors must be calibrated against laboratory-grade temperature standards at enough points to determine all of the constants in the model equation selected. Good practice would suggest one redundant calibration point to provide a closure check.

When an application requires more precision than provided by the manufacturer's tables but less than the highest achievable, a transfer standard instrument can be used. A strain-free platinum resistance thermometer or a quartz crystal thermometer can be used as such a transfer standard. Typically, the comparison is made in a well-stirred, temperature-regulated oil bath or in a comparison block of nickel or copper in an electrically heated oven.

Values of resistance and resistance divided by resistance at 0°C are listed in Table 9 for two typical commercial probes as functions of temperature (°C) and $1/T$ (K).

5 OPTICAL METHODS

Optical temperature measurements have become increasingly reliable and accurate as the electronic arts have advanced. This is especially true in the range below 600°C. Above 600°C, radiation methods have long enjoyed a position of trust in the measurements community. Low-temperature data interpretation and analysis that were once only conceptually possible can now be routinely handled with on-board computing.

There was a veritable explosion of instruments for optical temperature measurement in the period between 1980 and 2000. Only a few of the many types of optical temperature-sensing systems will be discussed here.

Bigelow et al.[48] describe the characteristics of commercial radiation temperature detectors for the range −173 to +3750 K and estimate the accuracy as between 0.5 and 1.5% of

Copyrighted Material

Copyright © 2006 John Wiley & Sons Retrieved from: www.knovel.com

Table 9 Resistance and Relative Resistance of Typical Probes

		Probe 1		Probe 2	
Temperature (°C)	$1/T$ (K)	Resistance	Relative Resistance	Resistance	Relative Resistance
−80	.00518	1660000	225.6968	2211000	225.7044
−70	.00493	702300	95.4861	935600	95.5084
−60	.00469	316500	43.0320	421500	43.0278
−50	.00448	151050	20.5370	201100	20.5288
−40	.00429	75790	10.3046	101000	10.3103
−30	.00412	39860	5.4194	53100	5.4206
−20	.00395	21870	2.9735	29130	2.9737
−10	.00380	12460	1.6941	16600	1.6946
0	.00366	7355	1.0000	9796	1.0000
10	.00353	4482	.6094	5971	.6095
20	.00341	2814	.3826	3748	.3826
30	.00330	1815	.2468	2417	.2467
40	.00319	1200	.1632	1598	.1631
50	.00310	811.30	.1103	1081	.1104
60	.00300	560.30	.0762	746.30	.0762
70	.00292	394.50	.0536	525.40	.0536
80	.00283	282.70	.0384	376.90	.0385
90	.00275	206.10	.0280	274.90	.0281
100	.00268	152.80	.0208	203.80	.0208
110	.00261	115	.0156	153.20	.0156
120	.00254	87.70	.0119	116.80	.0119
130	.00248	67.80	.0092	90.20	.0092
140	.00242	53	.0072	70.40	.0072
150	.00236	41.90	.0057	55.60	.0057

reading depending on the temperature level. The accuracy is better at high temperatures. These devices are vulnerable to errors from several sources: calibration, size of source, emissivity uncertainty, background radiation (especially in the lower temperature ranges), and gas path absorption of the infrared by water vapor or CO_2.

One way to avoid gas path absorption and source emissivity uncertainty is to use a blackbody cavity source and transmit the energy via a closed optical path. This is the principle behind the fiber-optic blackbody-sensing system described by Dils.[49] A fiber-optic blackbody radiation sensor measures the intensity of the radiation emitted from a blackbody cavity at the end of an optical fiber and deduces temperature from the intensity, using well-established laws of radiant emission.

The system has four main elements: the cavity, the high-temperature fiber, the low-temperature fiber, and the processor. Two of these elements are exposed to the high-temperature environment. A typical high-temperature fiber is a single-crystal sapphire fiber about 1.25 mm in diameter and usually between 100 and 250 mm long. The cavity can be formed by sputtering a thin metallic film onto the end of the sapphire fiber, typically about 5 μm. The metal layer can be covered by a film of alumina (also about 5 μm) to protect it from oxidation or erosion.

The general arrangement and the principal features of the data interpretation are shown in Fig. 25.

The cavity radiates as a ''dark-gray body'' (almost a blackbody) and the high-temperature fiber conducts the radiant energy from the cavity to the low-temperature fiber,

Copyright © 2006 John Wiley & Sons Retrieved from: www.knovel.com

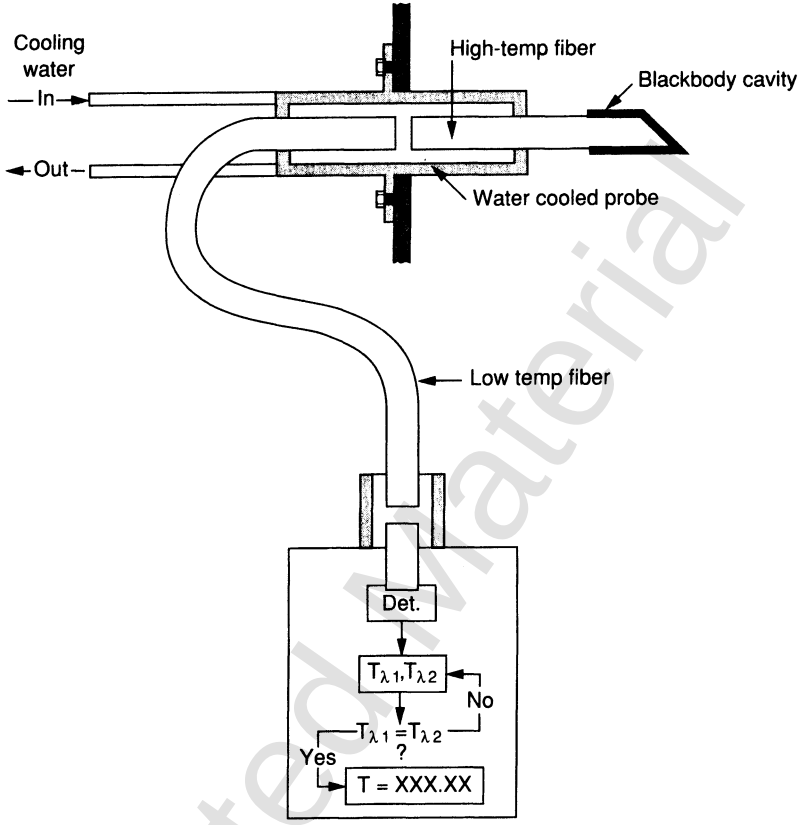


Figure 25 Fiber-optic radiation probe.

which in turn delivers it to the signal processor. The low-temperature fiber can be of great length, without degrading the signal, since loss coefficients for the low-temperature fiber material are quoted in percent per kilometer.

The processing of the radiant signal can be discussed in terms of the system pattern function: a set of equations that show how the system is supposed to work. The pattern function for the fiber-optic system is presented below. A final calibration adjusts the output to bring it into conformance with the calibration results.

$$I'(T_i) = \int_0^\infty \frac{C_1 C_d(\lambda, T_i)}{\lambda^5[\exp(C_2, \lambda T) - 1]} F(\lambda)\mathrm{BS}(\lambda, T_i)\mathrm{LTF}(T_i)\, d\lambda \tag{16}$$

and

$$I = I' K_{\text{sensor}} K_{\text{cable}} K_{\text{detector}} F(T_i) \tag{17}$$

where $I'(T_i)$ = detector current, pattern function
$I(T_i)$ = actual detector current, corrected for T_i
λ = wavelength
T = temperature, K
T_i = temperature of signal processor box
C_1 = radiation constant: 3.743×10^8, $\mathrm{W}\cdot\mu\mathrm{m}^4/\mathrm{m}^2$

Copyrighted Material

Copyright © 2006 John Wiley & Sons Retrieved from: www.knovel.com

C_2 = radiation constant: 1.4387×10^4, μm·K
$C_d(\lambda, T_i)$ = calibration constant for photodiode
$F(\lambda)$ = narrow-bandpass filter function
$\mathrm{BS}(\lambda, T_i)$ = beamsplitter function
$LTF(T_i)$ = low-temperature fiber transmission function

The dependence on T_i reflects changes in the optical properties of the mirrors and prisms used in steering the beams to their respective sensors.

The temperature range is 600–2000°C. Accuracy begins to fail at lower temperatures, while the sapphire fiber cannot tolerate higher temperatures.

The calibration precision is limited only by the precision with which the electrical signals can be read, assuming the equation governing the radiant emission to be absolutely accurate. The measurement accuracy depends on how well the sensor is brought into equilibrium with the specimen temperature.

The fiber-optic probe is sensitive to all the usual installation errors, which could be calculated from its physical and thermal properties. But it introduces one new concern: radiation loss along the transparent fiber. This is not an error mode that has been recorded in the literature, but it amounts to only a small fraction of the sensor's total radiation error under usual conditions. In addition, there is a small (3–10-K) error introduced because of radiation lost through the sides of the hot fiber near the cavity, the Brewster loss. These new error modes are not viewed as deterrents to the use of the probe as a reference system for high temperatures; rather they are part of the correction which must be applied at final calibration.

The sensing capsule is 1.25 mm in diameter and can be from 1 to 15 mm long. The optimum length is calculated on the basis of minimizing the radiation error of the cavity.

Standard thin-film units will respond to 10-kHz fluctuations in temperature. Response is flatter than that of a thermocouple, rolling off at only 3 dB per octave instead of 6.

Wickersham[50] developed a temperature-measuring system based upon the temperature sensitivity of the response of certain phosphors: fluor-optic temperature sensing. He found a family of phosphors whose fluorescent emission characteristics were strongly temperature dependent. Pulsing these phosphors with ultraviolet light resulted in an emission spectrum with two properties that depended on temperature: the ratios of amplitudes of certain bands and the decay times of the principal energy-containing bands. Two classes of instruments were then developed: ones that used the ratios of wavelengths and others that used the decay time. Experience favored the decay time instrument, and those are now the dominant type in the marketplace. Phosphors exist whose emissions are useful at temperatures of only a few kelvins, while others emit best in the range of 2000°C. Fluor-optic temperature-measuring systems are under development for high-temperature measurements on aircraft engine components and also for low-temperature measurements in systems with high magnetic fields or electric fields. Considerable development has proceeded on phosphors.[51] Since the sensor is an optical fiber, the system is not vulnerable to electromagnetic interference (EMI) and does not present a shock hazard to the operator.[52] Recent developments have focused on the illumination scheme, searching for more efficient coupling of the source and the phosphor by using blue light-emitting diodes (LEDs) as the illuminant source.[53]

Thermo-chromic liquid crystals have been used for mapping temperature fields in low-temperature systems (room temperature up to 100°C). These coatings have a reversible reaction to temperature change. Colorless below their lowest transition temperature, they display red when heated to the bottom of their range, with their color moving through the spectrum to blue at their highest active temperature. The full range of colors can be compressed into a temperature band of 1°C (narrow-band material) or stretched out over 10°C

Copyrighted Material

Copyright © 2006 John Wiley & Sons Retrieved from: www.knovel.com

(wide-band material). Narrow-band paints can be mixed; as long as the active bands do not overlap, the calibration of each band is unaffected by the presence of the other materials. A mixture of narrow-band materials painted on a surface will display a set of rainbow-colored lines representing isotherms centered around each active band. A wide-band paint displays a gradual shift in hue from one end of the range to the other. Digital image processing is required for interpretation of the wide-band images, especially when the incident light may change its spectrum over time, as discussed by Farina et al.[54] Liquid crystal material can be suspended in water and used to make visible the temperature distribution in the water.[55] If a liquid crystal is painted on a surface with known heat release per unit area, then the surface temperature distribution can be interpreted to learn the heat transfer coefficient distribution.[56]

Rajendran et al.[57] described a novel optical temperature measurement sensing system based on time-domain reflectometry. A long optical fiber was etched with 150 Bragg gratings regularly spaced along the fiber. The fiber was then embedded in the stator windings of an electric motor, along with a reference set of resistance–temperature detectors. The fiber was then pulsed from one end and time-domain reflectometry, using the back-scattered light from the gratings, was used to infer the temperature distribution along the fiber. The optical measurements agreed with the RTD measurements within ± 3°C over the length of the fiber. Many features of the distribution were evident in the optical measurements that were not visible in the RTD measurements since only a few RTDs were installed. An acoustic counterpart to this technique in described in Section 7.

6 ELECTRON NOISE THERMOMETERS

The electron noise method of temperature measurement uses for its signal the voltage developed by thermal agitation of the electrons in a resistor. The voltage is small (on the order of microvolts) and at high frequencies (up to 1 GHz). But, of greatest importance, the signal is linearly related to the absolute temperature (for frequencies less than kT/h, defined later) by a known physical law. Furthermore, the voltage is independent of the resistor material. The signal using multiple measurements can be made independent of the resistor value and insensitive to background noise (electrical noise). The signal is broadband with a zero mean and a high bandwidth. These characteristics allow rejection, by filtering, of environmental noise without loss of measurement accuracy.

The theory is described by Decreton et al.[58]

Electric noise due to thermal agitation was first described by Nyquist (1928)[59] and Johnson (1928)[60] An unloaded passive network always presents at its ends a voltage V_n fluctuating statistically around zero. This mean-squared noise voltage is given by

$$\overline{V_n^2} = 4kTR \frac{(hf)/(kT)}{\exp[(hf)/(kT)] - 1} \tag{18}$$

where h and k are Planck's and Boltzmann's constants respectively, T the absolute temperature, f the frequency, and R the resistance. For temperatures above 100 K and frequencies below 1 GHz, Eq. (18) can be accurately approximated by

$$\overline{V_n^2} = 4kTR \tag{19}$$

Equation (19) represents a frequency-independent white-noise signal. In a practical measurement, a given frequency bandwidth (df) is imposed, and the true rms voltage V_n is then given by

Copyrighted Material

Copyright © 2006 John Wiley & Sons Retrieved from: www.knovel.com

$$V_n = (4kTR\ df)^{(1/2)} \tag{20a}$$

When the current I_n is measured instead of the voltage, the equivalent model of the noise signal gives the rms current

$$I_n = \left(\frac{4kTdf}{R}\right)^{(1/2)} \tag{20b}$$

On multiplying Eqs. (20a) and (20b), the noise power P_n is obtained:

$$P_n = 4kT\ df \tag{21}$$

which is independent of the resistance value and thus is strictly linearly related to the absolute temperature.

Sophisticated signal extraction techniques are required. This technique is useful mainly at the temperature extremes (very low and very high) when other sensors fail. The technique is promising. Results have been reported up to 1000°C with errors less than 0.5% of reading over a period of several months.[61]

Brixy et al.[62] place a high degree of confidence on noise thermometry since "it is the only method of contact thermometry that is not affected by the unavoidable changes in the sensor at high temperatures." They describe the use of noise thermometry as the reference method in a study to determine the drift characteristics of WRe thermocouples at temperatures up to 2000°C.

7 ACOUSTIC VELOCITY PROBES

The velocity of stress-wave propagation through a gas, liquid, or solid can be used to measure temperature. In gases and liquids, the acoustic velocity is used (normal stress or pressure-wave propagation), whereas both normal and shear stress waves have been used in solids. Two signal-processing techniques are available: detection of resonance and measurement of the time of travel. These techniques have been used in both gases and solids, as described by Tasman and Richter.[63]

The acoustic velocity in a perfect gas is given by

$$a = \left[\left(\frac{C_p}{C_v}\right)RT\right]^{1/2} \tag{22}$$

Where C_p and C_v are the specific heats at constant pressure and at constant volume, respectively, R is the gas constant, and T is the temperature. Shear stress waves are not present in gases.

The normal stress propagation velocity in a solid (the extensional wave velocity) is

$$V_{\text{ex}} = \left(\frac{E}{D}\right)^{1/2} \tag{23}$$

where E and D are the modulus of elasticity and the density, respectively.

The shear stress propagation velocity in a solid is

$$V_{\text{sh}} = K\left(\frac{G}{D}\right)^{1/2} \tag{24}$$

where K is a shape factor and G and D are the shear modulus and density, respectively. Torsional waves sent down a cylindrical rod are one embodiment of shear waves. The

Copyrighted Material

Copyright © 2006 John Wiley & Sons Retrieved from: www.knovel.com

Hewlett-Packard quartz crystal thermometer uses shear-wave propagation in the resonance mode to achieve its very high precision (on the order of 0.0001 K).[64]

Tuning-fork resonance probes of pure sapphire have been run at 2000°C in a laboratory environment with an apparent stability of 1% or better by Bell et al.[65]

While capable of high precision under favorable conditions, the resonance mode is very sensitive to deposits or accidental contact between the resonator and its support. It is also inherently a line-averaging technique since it is the temperature of the oscillating stem, not that of the mass at the end, that determines the resonant frequency. For those reasons, most acoustic velocity systems proposed for high-temperature work use the time-of-flight technique known as the *pulse-echo* technique.

Tasman and Richter[63] offer the following description of the pulse-echo system:

> The pulse-echo technique measures the transit time of a single sound pulse through a thin wire. A magnetostrictive transducer transforms an electrical pulse into a sound pulse, which is injected into a transmission line. Discontinuities in the line, and the end of the line, reflect (part of) the sound pulse, which is then converted back into electrical signals by the transmitting transducer. The actual sensor is the wire joining the discontinuities. Almost any kind of discontinuity will do to produce an echo, even a kink in the wire. One sensor may contain several discontinuities, apart from its end, and thus measure the longitudinal temperature profile over several consecutive sections.

For good resolution, the sensor material should have a large change in propagation velocity over the temperature range to be encountered. Thoriated tungsten is one candidate material. Tasman and Richter quote the round-trip time difference between echos as increasing from about 4.5 to about 5.5 μs/cm when the temperature changes from 20 to 2700°C. Time differences can be measured to about ± 1 ns, which means that a 50-mm-long sensor could resolve temperature to ± 0.2 K at 2000°C (in theory). Practical considerations seem to limit the resolution to about ± 3 K for the 50-mm sensor. Tungsten is very sensitive to oxidation at high temperatures, and pure tungsten cannot be used as an acoustic velocity sensor because it continues to recrystallize at high temperatures, causing a continuous shift in calibration. Thoria blocks the grain growth, however, and the calibration of thoriated tungsten is stable (in the absence of oxygen).

8 TEMPERATURE-SENSITIVE COATINGS

Paints and crayons are available that are designed as temperature indicators,[66] up to 2500°F (1371°C) with a quoted accuracy of $\pm 1\%$. Two types are available: phase change and color change. When the phase change materials melt, they yield easily discernible evidence that their event temperature has been exceeded. Color change materials are subtler and less easy to interpret. There have been some complaints of calibration shifts of these paints when used on heavily oxidized materials which are believed due to alloying of the oxide with the paint.

These paints are nonmetallic and, therefore, have different radiation properties than metals. They should be used only over small areas of metallic surfaces (small compared with the metal thickness), or else their different emissivities will lead to a shift in the operating temperature of the parts. Since nonmetals tend to have higher emissivities than metals, the painted regions may have different radiation properties than the substrate material. Trial specimens should be checked if precise data are needed. If the specimens are to be heated by radiation from a high-temperature source, the different radiation properties can have a significant effect (2–3% in temperature).

Paints are useful in examining the distribution of temperature over a surface. Discrete spots should be used, rather than lines, since contact with molten material facilitates the melting of neighboring material even if it has not yet reached its own melting point.

Copyright © 2006 John Wiley & Sons Retrieved from: www.knovel.com

The paints are cheap and easy to apply. They provide a good ''first-look'' capability.

The principal disadvantages of the paints and crayons are that they require visual interpretation and they are one-shot, irreversible indicators. They read peak temperature during the test cycle, yet they cannot record whether the peak was reached during steady state or during soak-back.

9 FLOW RATE

The objective of flow rate measurement is to determine the quantity of matter flowing. In some instances a flowmeter returns this information directly, but in most cases the flowmeter signal is derived from some property of the flow: volume, heat transfer rate, momentum flux, and so on. In most cases the flowmeter signal requires correction for pressure, temperature, or viscosity before the flow rate is known.

Interest in mass flow rate stems from a basic principle of engineering: The creation rate of mass is zero. If a flow is measured in mass flow units, then unless the pipe leaks or more fluid is added, the mass flow rate is the same everywhere along the pipe, regardless of changes in the density of the fluid flowing. This is not so for a volume-based measurement. The volume flow rate represented by a fixed mass flow rate of gas depends upon the molecular weight, the temperature, and the pressure of the gas. Hence, as either T or P change, the volume flow measure would change, even though the mass flow measure remained constant.

The term *SCFM* (*standard cubic feet per minute*) is frequently used in gas flow metering. The number of SCFM corresponding to a particular flow rate is a measure of the volume flow rate that would have been observed had the same mass flow rate of the same gas occurred at standard conditions of temperature and pressure. In other words, it is the volume flow rate that the actual mass flow rate would have produced had it been delivered at standard temperature and pressure.

9.1 Nomenclature

Mass. Quantity of matter. When weighed under standard gravitational conditions (i.e., on the average surface of the earth), one pound mass weighs one pound (exerts a force of one pound) and 1 kg exerts a force of 9.8 N. Symbol: lb_m or kg.

Mass Flow Rate. The rate at which matter passes the measuring location. Pounds mass (or kg) per unit time. Symbol: W or $\dot{m}$ depending on the author.

Volume Flow Rate. The volume occupied by the mass passing the measuring location. Cubic feet (or cubic meters) per unit time. Symbol: Q.

Standard Conditions. An arbitrarily chosen pair of values (different organizations may use different values) for temperature and pressure used to describe a standard state for measurement of the density of a gas. (e.g., 70°F and 14.7 psia or 20°C and 760 mm Hg).

Standard Density (. . . of a gas). The density (lb_m per cubic foot or kg/m^3) of the gas in question when its temperature and pressure are those of standard conditions.

The following symbols and terms are commonly used in flow-metering situations. In the rate statements that follow, the time base is taken as minutes or seconds.

Copyrighted Material

Copyright © 2006 John Wiley & Sons Retrieved from: www.knovel.com

W = mass flow rate, lb_m/min or kg/s
Q = volume flow rate, ft^3/min or m^3/s

Also frequently used:

GPM = gallons per minute
CFM = cubic feet per minute
ACFM = actual cubic feet per minute, ft^3/min
SCFM = standard cubic feet per minute, ft^3/min

Consider a flowmeter operating at 2 atm and 70°F. The density of a gas at those conditions is twice its density at standard conditions. Consider a flow through the meter such that 100 ft^3 of gas at 70°F and 2 atm passes through the meter each minute. This 100 ft^3 of gas would occupy 200 ft^3 if it were at standard conditions. In this case, the flow rate could be described either as 100 ACFM (at 70°F and 2 atm) or 200 SCFM. If ACFM is quoted, then the temperature and pressure must also be specified. The term *SCFM* describes the mass flow but expresses it in terms of the volume that that mass flow would occupy if it were at standard conditions.

9.2 Basic Principles Used in Flow Measurement

Measurement of flow rate can be accomplished using many different physical principles. The basic flow rate equation is

$$W = \rho A V \tag{25}$$

where W = flow rate, lb_m/s (kg/s)
A = area, ft^2 (m^2)
V = velocity, ft/s (m/s)
ρ = density, lb_m/ft^3 (kg/m^3)

To measure flow, any metering system must provide enough information to evaluate all three terms. Usually, two of the terms are fixed, and flow is evaluated by observing the change in the remaining term. An orifice used on water (presumed to be constant density) fixes A and ρ, leaving W proportional to V. A variable-area meter fixes ρ and V, leaving W proportional to A. Any combination of physical laws that permits evaluation of ρ, A, and V can form the basis for a flow-metering system.

Flowmeters can be divided into three generic groups depending on their sensing principle: conservation based, rate based, and dynamic.

The first group consists of flowmeters which depend upon a conservation principle for their output. There are three conservation laws which can be related to mass flow: conservation of mass, conservation of momentum, and conservation of energy. Conservation of momentum provides the basis for a large class of meters: orifices, nozzles, Venturi meters, drag disks, and obstruction meters. Conservation of energy (usually thermal energy) has been used in the construction of flowmeters for small flow rate. The conservation-of-mass law is used implicitly in all systems.

The second large group of flowmeters depend upon *rate equations.* There are many natural phenomena whose rate depends upon fluid velocity: viscous drag, heat transfer, mass transfer, displacement of a tracer particle, and so on. Any rate process sensitive to flow rate can be used as the basis for a flowmeter.

Copyrighted Material

Copyright © 2006 John Wiley & Sons Retrieved from: www.knovel.com

The third class of flowmeters, the dynamic meters, contains those whose signal depends on some dynamic aspect of a flow field. This class of meters depends upon the repeatability of certain unstable behaviors of flow fields, for example, vortex precession in a swirling flow in an adverse pressure gradient and vortex shedding from a bluff body.

In the remaining sections the more common types of flowmeters will be discussed in terms of the following items: physical appearance, output data and peripheral equipment, equations computed for off-design operation, and sources for more information.

9.3 Orifice, Nozzle, and Venturi Meters

Orifice, nozzle, and Venturi meters are momentum-based, fixed-area meters. The flow-related signal reveals the pressure difference between two points on the meter body, as shown in Fig. 26. These meters accelerate the fluid stream by imposing a contraction on the flow area and then decelerate the flow by expanding back to the initial pipe diameter. As the fluid accelerates, its static pressure goes down. As it decelerates, the pressure rises again but not without loss. Losses are related to irreversibilities in the flow field, such as eddy structures and turbulence. Mechanical energy dissipated by these mechanisms comes from flow work done by the main stream. As a result, there is a loss in total pressure.

A principal determinant of "Which meter to choose?" is the irrecoverable loss in pressure associated with the meter. As shown in Fig. 26, orifice meters have the largest loss for a given signal among these three candidates and Venturi meters have the smallest. As might be expected, Venturi meters are more expensive than orifice meters. *Fluid Meters—Their Theory and Application*[68] provides extensive data on the losses for different styles of orifice, nozzle, and Venturi meters and data on the precautions that must be observed in installing them.

Measurement of flow rate with these meters requires two pressure sensors and one temperature sensor. The accuracy of the flow rate measurement will depend upon the accuracy of these instruments.

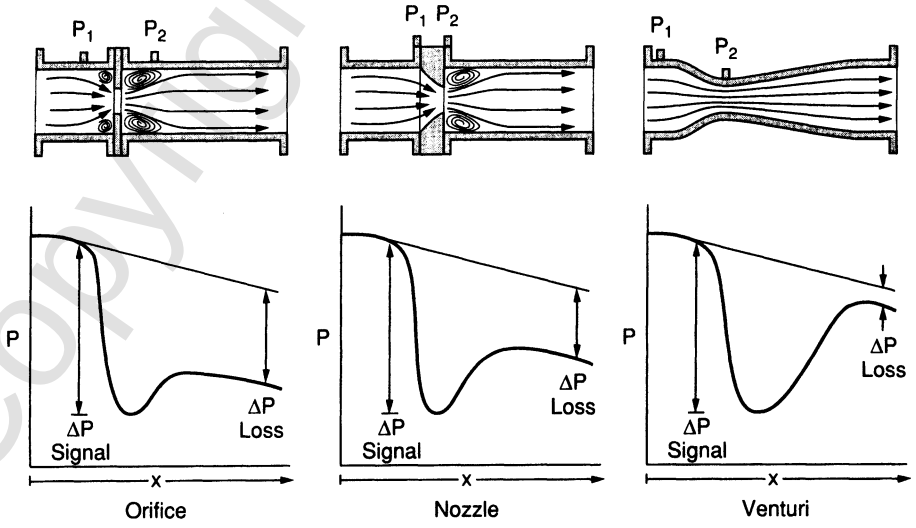


Figure 26 Orifice, nozzle, and Venturi meter pressure distributions. (From Ref. 67, with permission.)

Copyrighted material

Copyright © 2006 John Wiley & Sons Retrieved from: www.knovel.com

The equation given below takes its nomenclature from the previous reference:

$$W_h = 359CFd^2F_aY\sqrt{h_w\gamma} \tag{26}$$

where W_h = flow rate, lb_m/h
C = coefficient of discharge, dimensionless
F = coefficient of approach, dimensionless
d = minimum diameter of the orifice, nozzle, or Venturi, in. (m)
F_a = coefficient of expansion, dimensionless
Y = compressibility factor, dimensionless
h_w = pressure difference $P_1 - P_2$, in. H_2O
γ = density of fluid flowing at location of measurement of P_1, lb_m/ft^3

Of the seven required terms, two are data or derived from data (h_w and γ), while five are calibration coefficients tabulated within the reference. The product of C and F is tabulated directly (K).

The coefficient K is a function of the flow rate; hence Eq. (26) cannot be solved explicitly—an iterative procedure is required. A first estimate of $K = C \times F = 0.60$ should be used for a first try. Using this K value, the calculated flow will generally be within a few percent and will serve to fix the exact value of K (within fractions of a percent).

It is apparent from Eq. (26) that the signal (ΔP) is proportional to W_n^2, the square of the flow rate. If the flow is fluctuating and an average ΔP is observed, then this corresponds to the time average of the square of the instantaneous flow, which is not equal to the square of the time-average flow. As a result, orifice, nozzle, and Venturi meters are not recommended for pulsating flows.

The most authoritative source of data regarding installation precautions for this class of meters is found in Reference 68. A good general reference is Benedict.[69]

In general, orifice flowmeters are accurate within $\pm 1/2\%$ of flow rate even without individual calibrations, when used properly. To achieve this accuracy, the orifice meter must be installed in strict compliance with the prescribed conditions for the approach and exit flow paths. The specifications in Ref. 68 cannot be abridged without loss of generality and should be treated as the final arbiter of an installation.

9.4 Variable-Area Meters

A variable-area meter consists of a tapered tube (usually of glass) with a float inside, as shown in Fig. 27. The clearance area between the outer diameter of the float and the inner diameter of the tube is a function of float position. When flow passes through the meter, it lifts the float under constant-pressure-drop conditions until the clearance area is sufficient to pass the existing flow. The output of the meter is *float position.* For gas flow measurements, pressure and temperature must be measured upstream of the float to establish the density.

Variable-area meters are usually purchased for use in a specific application and delivered calibrated for those conditions. The scale is calibrated directly in flow rate units. If the pressure and temperature of the flow remain at their design values, the float position gives flow rate directly.

A typical calibration legend for such a meter would read:

Full scale = 1.44 SCFM

Gas specific gravity of 1.38

When metered at 25 psig and 70°F

Copyrighted Material

Copyright © 2006 John Wiley & Sons Retrieved from: www.knovel.com

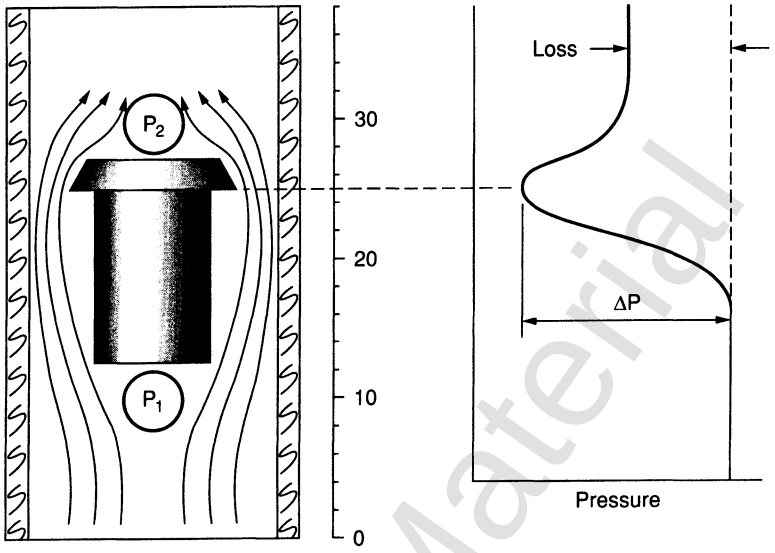


Figure 27 Variable area flowmeter pressure distribution. (From Ref. 67, with permission.)

The float position then directly reads in percentage of full-scale flow provided the inlet pressure is 25 psig, the inlet temperature is 70°F, and the specific gravity of the gas flowing is 1.38.

For off-design operation of the variable-area meter it is necessary to correct for changes in pressure, temperature, or specific gravity.

A sufficiently accurate equation for gas flow service can be derived from a force balance on the float in combination with Eq. (25), thus resulting in the fundamental equation for flow measurement

$$W_{USE} = W_{calib} \sqrt{\frac{\rho_{USE}}{\rho_{calib}}} \tag{27}$$

where W_{USE} = mass flow rate under actual conditions of use, lb_m/s (kg/s)
W_{calib} = mass flow rate under calibration conditions for same float position, lb_m/s (kg/s)
ρ_{USE} = density of fluid flowing, lb_m/ft^3 (kg/m^3)
ρ_{calib} = density of calibration fluid, lb_m/ft^3 (kg/m^3)

Example. Assume that the meter previously described is to be used in a new application where the fluid is air (Specific gravity = 1.00), the pressure is 100 psig, and the temperature is 70°F. What would be the full-scale flow rate in SCFM (air)?

$$W_{USE} = W_{calib} \sqrt{\frac{\rho_{USE}}{\rho_{calib}}}$$

$$\rho_{USE} = \frac{P_{USE}}{R_{AIR} T_{USE}} = \frac{(100 + 14.7)(144)}{53.3 \times (460 + 70)}$$

$$= 0.585 \ lb_m/ft^3$$

Copyrighted Material

Copyright © 2006 John Wiley & Sons Retrieved from: www.knovel.com

$$\rho_{\text{calib}} = 1.38 \left(\frac{P_{\text{calib}}}{R_{\text{AIR}} T_{\text{calib}}} \right)$$

$$= 1.38 \frac{(25 + 14.7)(144)}{(53.3)(460 + 70°\text{F})} = 0.279$$

$$W_{\text{calib}} = (1.44)(1.38)(.075) = 0.149 \text{ lb}_\text{m}/\text{s}$$

$$W_{\text{USE}} = (0.149) \sqrt{\frac{0.585}{0.279}} = 0.216 \text{ lb}_\text{m}/\text{s}$$

$$\text{SCFM}_{(\text{USE})} = \frac{W_{\text{USE}}}{\rho_{\text{STD,AIR}}} = \frac{W_{\text{USE}}}{0.075} = 2.877 \text{ SCFM}$$

This correction equation was derived under the assumption that the float was held up only by the pressure force (i.e., buoyancy and viscous drag were both negligible). When metering liquids of high density, the buoyant force must be accounted for, and if the viscosity of the fluid exceeds the *viscosity immunity ceiling* for a given meter, then the viscous drag must be taken into account. Precautions for dealing with these two cases are covered by the manufacturer's instructions. A meter purchased for gas service cannot be converted to liquid service by the preceding equation, or vice versa; a new calibration is required.

Variable-area meters are generally limited in accuracy to ± 1 or $\pm 2\%$ of full-scale reading.

It is important to measure the actual density of the fluid flowing in the meter to ensure that the calibration conditions are properly met. Pressure and temperature must be measured at the meter, just upstream of the float.

Irreversibilities involved in the mixing of the annular jet introduce losses in pressure that are nearly independent of flow rate and roughly equal to the pressure required to hold up the float. More accurate meters generally have higher losses (up to 3 or 4 psi used with air).

9.5 Laminar Flowmeters

Commercial laminar flowmeters consist of a *matrix* or *core* of small-diameter passages arranged so that the pressure drop across this core can be measured. The meter must be sized properly so the flow in these passages will remain laminar, even at the highest rated flow. If the flow remains laminar, then the pressure drop is linearly related to the volume flow rate through the core. General commercial practice is to provide flow-straightening sections upstream and downstream of the core and measure the pressures in the space between the flow straighteners and the core, as shown in Fig. 28.

Laminar flowmeters produce a pressure difference, usually 0–8 in. H_2O, which must be measured using an appropriate auxiliary instrument. The meter responds to volume flow; hence it is also necessary to measure the density of the fluid flowing. If the composition is known, density can be calculated knowing temperature and pressure at the inlet.

The pressure drop across a well-designed laminar flowmeter is linearly proportional to the volume flow rate (ACFM) multiplied by the viscosity of the fluid flowing. The pressure drop is independent of density.

Each meter is accompanied by a calibration curve, which typically reads:

> Air Flow in Cubic Feet per Minute at 70°F and 29.92 Inches of Mercury Absolute vs. Pressure Drop, Inches of Water.

Copyrighted Material

Copyright © 2006 John Wiley & Sons Retrieved from: www.knovel.com

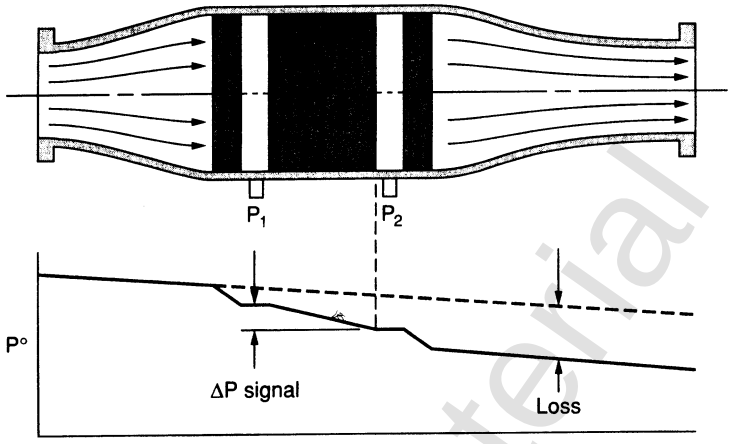


Figure 28 Laminar flowmeter pressure distribution. (From Ref. 67, with permission.)

The SCFM flow rate can be taken directly from the calibration curve if the meter is being used at 29.92 in. Hg and 70°F. If the pressure is 2 atm, however, then the density, the mass flow, and the number of SCFM corresponding to the same pressure drop signal would be doubled. Tables of pressure corrections, often provided with each meter, simplify this calculation.

If the temperature of the metered flow is higher than 70°F, the density is less than standard density and the viscosity of the flow is higher. Temperature correction factors, often provided in tabular form, account for both effects. The temperature correction factor for air flow is roughly proportional to absolute temperature raised to the 1.7 power, and it accounts for both the decrease in density and the increase in viscosity.

The equation for a laminar flowmeter in terms of the calibration chart is

$$\text{SCFM} = (\text{chart CFM})(CP)(CT)$$

or

$$\text{SCFM} = (\text{chart CFM})\left(\frac{P_{\text{act}}}{29.92}\right)\left(\frac{530}{460 + T_{\text{act}}}\right)^{1.7} \tag{28}$$

Laminar flowmeters respond linearly to flow; hence they can be used to directly measure the time average of a fluctuating flow. Commercial meters will usually average properly up to about 100 Hz.

9.6 Instability Meters

Two modern flow-metering systems derive their signal from the frequency of occurrence of an unstable fluid-dynamic phenomenon. One uses a swirling flow in a divergent passage to generate a precessing stall region. The other introduces a prismatic bluff body into a pipe and generates a periodic vortex trail. In each case, the frequency of the unstable event is related to the volume flow rate through the meter. Each claims 100:1 usable range, and each produces a pulse train whose repetition rate is linearly related to flow.

The Swirlmeter (registered trademark of the Fischer and Porter Co.) is shown schematically in Fig. 29. The meter has no moving parts. Stationary blades impart a swirling motion

Copyrighted Material

Copyright © 2006 John Wiley & Sons Retrieved from: www.knovel.com

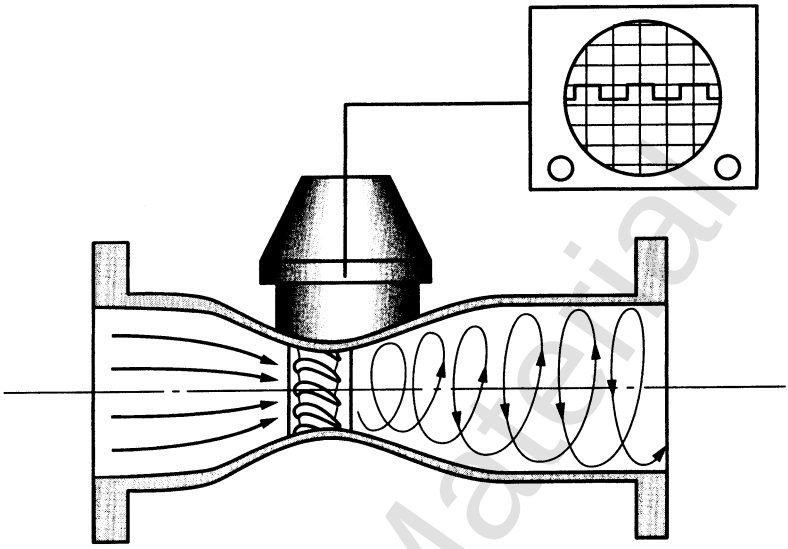


Figure 29 Swirlmeter (registered trademark, Fischer and Porter Co.). (From Ref. 67, with permission.)

to the flow, which then enters a diverging passage. The rotating flow field develops a stall (a region of relatively low axial velocity), which rotates in the diverging passage. An anemometer button in the wall senses the low-speed region each time it passes, generating a pulse train. The frequency of this pulse train is linearly related to the volume flow rate.

Mass flow rate calculation requires knowledge of the volume flow and the density. The equation is

$$\text{ACFM} = \frac{\text{total counts per minute}}{\text{calibration constant}} \tag{29}$$

$$W = \text{ACFM} \times \rho_{\text{act}} \tag{30}$$

$$\text{SCFM} = \text{ACFM} \times \frac{\rho_{\text{act}}}{\rho_{\text{STD}}} \tag{31}$$

Vortex-shedding flowmeters use a prismatic bluff body to generate the instability and one of several means to sense the oscillations of the stagnation streamline, which occur when the bluff body is shedding a vortex trail. A plan view schematic is shown in Fig. 30.

Again, these meters can operate over a turn-down ratio of 100:1 or better and claim $\pm 0.25\%$ accuracy.

The advantages of the instability meters are due to their pulse train signal, which is not easily obscured by random noise and can be transmitted over long distances.

9.7 Ultrasonic Flowmeters

An ultrasonic flowmeter is a device for estimating the flow rate in a duct based on measuring the propagation velocity of sound waves along one or more paths through the fluid, assuming the velocity profile in the duct to be known. There are two general types of ultrasonic flowmeters: transit time and Doppler. In both types, a transmitter unit injects an ultrasonic

Copyrighted Material

Copyright © 2006 John Wiley & Sons Retrieved from: www.knovel.com

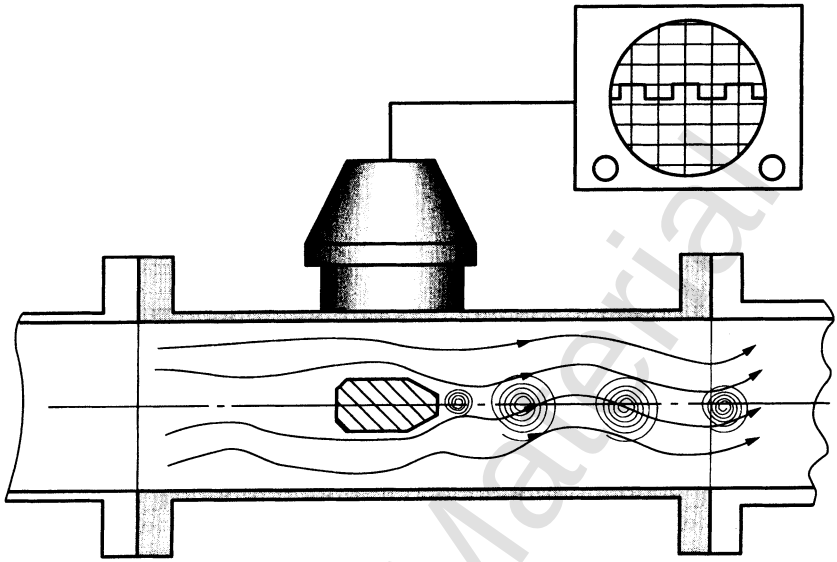


Figure 30 The vortex meter, schematically. (From Ref. 67, with permission.)

beam (an acoustic signal of at least 20 kHz or higher, more typically up to 1 MHz) into the fluid and a second unit receives the signal. The transmitter and receiver can be directly in contact with the fluid (a ''wetted'' system) or attached to the outside of the pipe wall (a ''clamp-on'' or ''nonwetted'' system).

Doppler Meter Principles

In a Doppler meter, the injected beam is reflected off particles, bubbles, or turbulence structures (very high frequency required) in the flow and picked up by the receiver. The frequency of the reflected beam is compared with the frequency of the injected beam and the flow rate inferred from the frequency shift and the system geometry. If all of the particles were moving at the same velocity V, that velocity could be determined from the frequency shift using the following equation[70,71]:

$$V = a \frac{\Delta f}{2f \cos \theta} \tag{32}$$

where V = velocity of particles
a = acoustic velocity in fluid
Δf = frequency shift
f = injected frequency
θ = angle between injected beam and pipe centerline

The velocity is not uniform across a pipe; hence a calibration factor must always be used. This factor will depend on the piping layout as well as the installation geometry of the flowmeter. Elbows, tees, and valves upstream of the measuring location will affect the velocity distribution and, therefore, the calibration factor. Doppler systems using very high frequency (around 1 MHz) can be used with clean, turbulent flows, but, for the most part, Doppler systems are used on flows with low to moderate (100-ppm) particle or bubble loading.

Copyrighted Material

Copyright © 2006 John Wiley & Sons Retrieved from: www.knovel.com

Yamanaka et al.[72] describe a velocity profile measuring technique using a time-domain correlation method which they claim has two advantages over the conventional pulse Doppler: higher time resolution and avoidance of the Nyquist limit on maximum velocity.

Transit Time Meter Principles

Transit time ultrasonic flowmeters are discussed by Lynnworth,[73] who traces the history of such meters back to the 1930s, and by Yoder[74] as part of a survey article. A transit time ultrasonic flowmeter compares the transit times of pulses transmitted upstream and downstream and infers the average fluid velocity along the beam path from the difference of the two transit times. Typically this is accomplished using pairs of transmitter–receiver units. Each unit serves alternately as a transmitter and a receiver, sending out a burst and then receiving a burst from the other unit. Commercial units are available.[75]

The time required for the pulse to travel from the upstream transmitter to the downstream receiver is shorter than the time required for the pulse originating at the downstream unit to move upstream, against the flow velocity. This time difference, Δt, is the basis for the flow measurement, as described in Efunda[76]:

$$\Delta t \triangleq (t_u - t_d) = \frac{L}{a - V\cos\theta} - \frac{L}{a + V\cos\theta} \tag{33}$$

$$= L\,\frac{2V\cos\theta}{a^2 - V^2\cos^2\theta} = \frac{\dfrac{2VX}{a^2}}{1 - (V^2/a^2)\cos^2\theta} \tag{34}$$

If $V/a << 1$ (flow Mach number $<<$ 1), then

$$\Delta t \approx \frac{2VX}{a^2} \tag{35}$$

$$V \approx \frac{a^2\,\Delta t}{2X} \tag{36}$$

where a = acoustic velocity in fluid
t_u = upwind transit time
t_d = downwind transit time
$\Delta t = t_u - t_d$
L = line-of-sight distance between transponders
θ = angle between line of sight and pipe centerline
V = fluid velocity (assumed uniform along line of sight)
X = axial distance between transponders, $L\cos\theta$

Flood[71] introduces an additional term to account for the transmission time of the pulse through the body of the transducer and the wall of the pipe, so that the calibration equation can be based on the overall time difference. Eq. (36) deals only with the transit times within the fluid and does not include the wall delay.

Both types of ultrasonic flowmeters use information gathered along the propagation path (or paths) to infer the average flow over the entire flow area, as though the velocity were uniform. Considerable effort has been put into the development of methods for dealing with nonuniform flow.

Nonuniform Velocity

The simplest nonuniformities to deal with are those found in isothermal, fully developed laminar or turbulent flows. These distributions are symmetric about the centerline and, if the

Copyrighted Material

Copyright © 2006 John Wiley & Sons Retrieved from: www.knovel.com

propagation path intersects the centerline, a simple Reynolds-number-dependent calibration factor could be used. Such flows are rare, however, in industry. More realistic flows present more complex nonuniformities. Pipe bends, elbows, and tees lying in one plane generate centrifugal forces that move the highest velocity fluid from the centerline of the pipe toward the outside of each turn. This movement, in turn, causes secondary flows that roll up into pairs of vortices near the inside walls of the turns. If the elbows and bends are ''out of plane,'' the resulting velocity distributions may have several local maxima, not just one. Such effects have been discussed by Ruppel and Peters,[77] who experimentally investigated the effects of several upstream piping configurations on the accuracy of an ultrasonic flowmeter. One approach to this problem has been to use several acoustic paths disbursed across the cross section of the pipe. Flowmeters with up to five paths have been tested. There are also different ways of ''weighting'' the data from the individual paths in forming the average.

A complex set of velocity distributions has been studied by Moore et al.[78] who used closed-form descriptions of representative multimodal velocity distributions (constant density) to challenge a family of multipath transit time flowmeter designs. These distributions were used as inputs to a program that calculated the ''reading'' of the flowmeter. These readings were then compared to the ''real'' flow deduced by integrating the velocity distribution over the flow area. Three different mathematical schemes were compared for weighting the readings from different paths as well as different numbers of acoustic paths from 2 to 5. For each flowmeter configuration, 90 trials were made, with the velocity profile being rotated 2 degrees each time. The range of calibration factors (maximum to minimum) for these 90 trials was recorded as a measure of the orientation sensitivity of the configuration. The authors offer this approach as a good tool for optimizing the design of multipath flowmeters.

Yeh et al.[79] combined a four-path transit time ultrasonic flowmeter with pattern recognition software and a ''learning algorithm.'' The system was ''educated'' on a set of experimental and computational flow fields and ''learned'' to recognize and accommodate flow fields and adjust its calibration according to the flow field it encountered.

Temperature Gradients

If there is heat transfer to or from the fluid, the resulting density gradient is capable of distorting the flow calibration even in a straight run of pipe with fully developed flow. In situations with bends, the distortions may be worse with heat transfer than the isothermal cases.

Willatzen[80] looked at the effect of the radial density gradient resulting from heat transfer out of a water flow with a fully developed parabolic velocity distribution. The author considered a system in which idealized (permeable) transducers of different diameters centered within the pipe generated ultrasonic waves. The smallest diameter transducers generated waves containing up to eight modes; the largest ($R/R_0 = 1$) produced only the fundamental mode. In the absence of density gradients, all modes except the fundamental overestimated the mean flow while excitation of the fundamental mode alone gave error-free measurements. The predicted error was zero when the transducer disks occupied the entire pipe cross section (fundamental mode only). With a radial temperature gradient in the water (heat transfer out of the fluid into the surroundings) the indicated flow was low by about 2% even with only the fundamental mode excited.

Pulsing Flow

Pulsations in the flow can cause errors if the pulsation frequency aliases with the meter pulse frequency. This topic has been treated by Berrebi et al.[81] and by Carlander and Delsing,[82] who reported experimentally measured errors of more than 2–4% induced by unsteady pres-

Copyright © 2006 John Wiley & Sons Retrieved from: www.knovel.com

sure pulsations and velocity profile disturbances downstream of compound, out-of-plane elbows and bends. Carlander and Delsing proposed using the variance in a set of measurements as a diagnostic clue to the existence of an error in the mean value, since an increased variance in indicated flow accompanied the onset of errors due to pulsations.

Aliasing with Process Noise

Vermeulen et al.[83] examined the error introduced by aliasing of the noise from a throttling control valve with the signal of an ultrasonic flowmeter. They report that, under certain predictable conditions, the ultrasonic component of noise from the control valve can be larger than the signal generated by a commercial ultrasonic flowmeter and, therefore, can swamp out the meter.

Non-Newtonian Fluids

Non-Newtonian fluids display velocity distributions that are significantly different from Newtonian fluids and, hence, would be expected to cause trouble with flowmeters that require an assumption of the profile shape. Fyrippi, Owen, and Escudier[84] tested a single-beam transit time ultrasonic flowmeter in a non-Newtonian fluid and found significant errors.

Turbulence

A fundamental assertion used in developing the equations for transit time flowmeters is that the flow field is the same during the up-wind and the down-wind pulse transits. This may not be the case in a turbulent flow. This possibility was investigated by Weber et al.[85]

Fouling

Lansing[86] Investigated the effect of fouling on the performance of a transit time ultrasonic flowmeter.

REFERENCES

1. NIST ITS90 Thermocouple Data base; www.nist.gov.
2. R. J. Moffat, *Experimental Methods in the Thermosciences,* Department of Mechanical Engineering, Stanford University, Stanford, CA, 1978, pp. 1–26.
3. R. J. Moffat, ''The Gradient Approach to Thermocouple Circuitry,'' in *Temperature, Its Measurement and Control in Science and Industry,* Charles M. Herzfeld (ed.), Vol. 3, Part 2, Reinhold New York, 1962, pp. 33–38.
4. R. J. Moffat, *Experimental Methods in the Thermosciences,* Department of Mechanical Engineering, Stanford University, Stanford, CA, 1980, pp. 2–3.
5. R. P. Benedict, *Fundamentals of Temperature, Pressure, and Flow Measurement,* 2nd ed., Wiley, New York, 1977.
6. E. O. Doebelin, *Measurement Systems: Application and Design,* McGraw-Hill, New York, 1966.
7. M. Campari and S. Garribba, ''The Behavior of Type K Thermocouples in Temperature Measurement: The Chromel-P-Alumel Thermocouple,'' *Review of Scientific Instruments* **42**(5), 644–653 (May 1971).
8. R. E. Bentley, ''Thermoelectric Hysteresis in Nickel-Based Thermocouple Alloys,'' *Journal of Physics D: Applied Physics* **22,** 1902–1907 (1989).
9. W. Schuh and N. Frost, ''Improving Industrial Thermocouples Temperature Measurement,'' *NEWS 2002,* www.watlow.com.
10. R. E. Bentley and T. L. Morgan, ''Thermoelectric Effects of Cold Work in Pt/10%Rh and Pt/13%Rh versus Pt Thermocouples,'' *Metrologia* **20**(2), 61–66 (June 1984).
11. O. A. Geraschenko and N. N. Ionova, ''Thermal EMF of Plated Thermocouples'' UDC 536,532, Translated from *Ismeritel'naya Tekhnika,* No. 1, January 1966, pp. 65–66.

Copyrighted Material

Copyright © 2006 John Wiley & Sons Retrieved from: www.knovel.com

12. C. Tallman, personal communication, 1964.

13. W. Gill and J. T. Nakos, ''Temperature/Heat Flux Errors Caused by High Temperature Resistive Shunting along Mineral-Insulated, Metal Sheathed Thermocouples,'' *ASME HTD* **364-4,** 43–56 (1999).

14. R. J. Moffat, unpublished research results, 2002.

15. A. A. Sachenko, V. V. Kochlan, and V. Y. Mil'chenko, ''Check of Thermoelectric Transducers with Built-in Temperature Calibrators,'' *Measurement Techniques* (English translation of *Izmeritel'naya Tekhnika*) **31**(7), 679–682 (December 1988).

16. H. M. Hashemian, ''In-Situ Response Time Testing of Thermocouples,'' in *Proc. 1989 International Instrumentation Symposium,* 35th, Orlando, FL, May 1–4, 1989. ISA, Research Triangle Park, NC, pp. 587–593.

17. C. Y. Yang and D. W. Clarke, ''A Self-Validating Thermocouple,'' *IEEE Transactions on Control Systems Technology* **5**(2), 239–253 (March 1997).

18. R. J. Moffat, ''Gas Temperature Measurement,'' in *Temperature, Its Measurement and Control in Science and Industry,* Vol. 3, Part 2, Reinhold, New York, 1962, p. 553.

19. D. Elmore and W. B. Watkins, ''Dynamic Gas Temperature Measuring System,'' *ISA Transactions* **24**(2), 73–82 (1985).

20. R. J. Moffat, ''A Transient Method for Measuring Very High Gas Temperature,'' *ISA Proceedings of the International Instrumentation Symposium,* **47,** 413–422 (2001).

21. G. T. Lalos, ''A Sonic Flow Pyrometer for Measuring Gas Temperatures,'' *Journal of Research National Bureau of Standards* **47,** 179–190 (1951), RP2242.

22. O. P. Norton, R. Arunkumar, and R. L. Cook, ''Suction Thermocouple Measurements in High Temperature Gas Streams,'' *ISA Proceedings of the International Instrumentation Symposium,* **47,** 451–459 (2001).

23. R. J. Moffat, ''Gas Temperature Measurement: A Two-Sensor Method for Canceling Radiation Error,'' *ISA Proceedings of the International Instrumentation Symposium,* **47,** 405–412 (2001).

24. S. Brohez, C. Delvosalle, and G. Marlair, ''A Two-Thermocouple Probe for Radiation Corrections of Measured Temperatures in Compartment Fires,'' *Fire Safety Journal* **39**(5), 399–411 (July 2004).

25. L. G. Blevins and W. M. Pitts, ''Modeling of Bare and Aspirated Thermocouples in Compartment Fires,'' *Fire Safety Journal* **33**(4), 239–259 (1999).

26. W. M. Pitts, E. Braun, R. D. Peacock, H. E. Mitler, E. L. Johnsson, P. A. Reneke, and L. G. Blevins, ''Temperature Uncertainties for Bare-Beaded and Aspirated Thermocouple Measurements in Fire Environments'' Special Technical Publication No. 1427, American Society for Testing and Materials, West Conshohocken, PA, pp. 3–15.

27. R. J. Moffat, ''A Proposed Temperature Probe for Inter-Stage Compressor Measurements,'' *ISA Proceedings of the International Instrumentation Symposium,* **47,** 423–430 (2001).

28. R. Vasquez and J. M. Sanchez, ''Temperature Measurement System for Low Pressure Ratio Turbine Testing,'' in *ASME Turbo Expo 2003: Power for Land, Sea, and Air,* Vol. 1, ASME International Gas Turbine Institute, Atlanta, GA, June 16–19, 2003, pp. 527–539.

29. N. R. Keltner and J. V. Beck, ''Surface Temperature Measurement Errors,'' *ASME Transactions, Journal of Heat Transfer,* **105,** 312–318 (May 1983).

30. K. B. Sobolik, N. R. Keltner, and J. V. Beck, ''Measurement Errors for Thermocouples Attached to Thin Plates. Application to Heat Flux Measurement Devices,'' *ASME HTD* **112,** 15–22 (1989).

31. P. C. Han and X. X. Wei, ''Film Thermocouple Technique for Measurement of Nonmetal Surface Temperature,'' in *Proceedings of the International Centre for Heat and Mass Transfer,* 1991, pp. 137–144.

32. A. M. Osman, L. H. Eilers, and J. V. Beck, ''Correction of Surface Temperature Measurements using an Inverse Method,'' in *Proceedings of the International Conference on Inverse Problems in Engineering,* 1998. pp. 599–606.

33. Omega Engineering, *Temperature Measurement Handbook and Encyclopedia,* Stamford, CT, 1984, pp. El–E18.

34. Product Bulletin 2086, Rosemount Engineering, Chanbassan, MI, rev. October 1978.

35. Product Bulletin 2108, Rosemount Engineering, Chanbassan, MI, rev. June 1974.

36. C. W. Lewis, ''Four-wire Techniques Minimize Temperature Measurement Errors,'' *InTech* **42**(5), 40–43 (1995).

Copyrighted Material

Copyright © 2006 John Wiley & Sons Retrieved from: www.knovel.com

37. H. N. Norton, *Sensor and Analyser Handbook,* Prentice-Hall, Englewood Cliff, NJ, 1982, p. 337.

38. R. P. Benedict, *Fundamentals of Temperature, Pressure, and Flow Measurement,* 2nd ed., Wiley, New York, 1977, pp. 38–9.

39. Technical Bulletin MCT-18l, Victory Engineering Corporation, Springfield, NJ, 1968.

40. ''YSI Precision Thermistor Products,'' Yellow Springs Instrument Co., Yellow Springs, OH, 1980.

41. K. Park, ''Improvement in Electrical Stability by Addition of SiO 2 in $(Mn_{1.2}Ni_{0.78}Co_{0.87}Cu_{0.15}Si_x)O_4$ Negative Temperature Coefficient Thermistors,'' *Scripta Materialia* **50,** 551–554 (2004).

42. M. Tagawa, K. Kato, and Y. Ohta, ''Response Compensation of Thermistors: Frequency Response and Identification of Thermal Time Constant,'' *Review of Scientific Instruments* **74**(3), 1350–1358 (2003).

43. *Temperature Measurement Handbook and Encyclopedia,* Omega Engineering, Stamford, CT, 1985, pp. T75–T76.

44. J. S. Steinhart and S. R. Hart, ''Calibration Curves for Thermistors,'' *Deep Sea Research* **15,** 497 (1968).

45. A. S. Bennet, ''The Calibration of Thermistors over the Temperature Range of 0–30°C,'' Deep Sea Research, **19,** 157 (1972).

46. L. Seren, C. B. Panchal, and D. M. Rote, ''Temperature Sensors for OTEC Applications,'' ANL/OTEC-PS-12, Argonne National Laboratory, U.S. Department of Energy, May 1984.

47. G. Bosson, F. Guttmann, and L. M. Simmons, ''A Relationship between Resistance and Temperature of Thermistors,'' *Journal of Applied Physics* **21,** 1267–1268 (1950).

48. R. N. Bigelow, P. S. Carlson, A. M. Hunter, and S. R. King, ''Radiation Thermometry,'' in *Measurement Science Conference Proceedings,* 1996.

49. R. R. Dils, ''High Temperature Optical Fiber Thermometer,'' *Journal of Applied Physics* **54,** 1198–1201 (1983).

50. K. A. Wickersham, ''New Thermometry Technique Measures Component Temperature,'' in *Electronic Packaging and Production,* Cahners Publishing, September 1981.

51. D. M. Cunningham, S. W. Allison, and D. B. Smith, ''Thermographic Properties of Eight Blue-Emitting Phosphors,'' ISA 1993, Paper No. 93-111, in *Proc. 39th Int. Inst. Symp.* Albuquerque, NM, May 1993.

52. S. C. Jensen, S. D. Tilstra, G. A. Barnabo, D. C. Thomas, and R. W. Phillips, ''Fiber Optic Temperature Sensor for Aerospace Applications,'' in *Proceedings of SPIE,* Vol. 1369, International Society for Optical Engineering, 1991, pp. 87–95.

53. R. Raja and G. T. Cunningham, ''Experimental Investigation of Phosphor Thermography Using a Blue LED optical excitation Source,'' in *ISA TECH/EXPO Technology Update Conference Proceedings,* Vols. 424–425, 2002, pp. 1085–1092.

54. D. Farina, J. Hacker, J. K. Eaton, and R. J. Moffat, ''Illuminant Invariant Calibration of Thermochromic Liquid Crystals,'' paper presented at the ASME National Heat transfer Conference, August 8–11, 1993.

55. H. S. Rhee, J. R. Koseff, and R. L. Street, ''Flow Visualization of a Recirculating Flow by Rheoscopic Liquid and Liquid Crystal Techniques,'' *Experiments in Fluids* **2,** 57–64 (1984).

56. K. Hollingsworth, A. L. Boehman, E. G. Smith, and R. J. Moffat, ''Measurement of Temperature and Heat Transfer Coefficient Distributions in a Complex Flow Using Liquid Crystal Thermography and True-Color Image Processing,'' Collected Papers in Heat Transfer, *ASME HTD* **123,** 35–42 (1989).

57. V. Rajendran, M. Deblock, T. Wetzel, M. Lusted, C. Kaminski, and B. Childers, ''Use of Fiber Optic Based Distributed Temperature Measurement System for Electrical Machines,'' *Proceedings of SPIE—The International Society for Optical Engineering;* **5191,** 214–225 (2001).

58. M. Decreton, L. Binard, C. Delrez, W. Hebel, and W. Schubert, ''High-Temperature Measurements by Noise Thermometer,'' *High Temperature—High Pressure,* **12,** 395–402 (1980).

59. H. Nyquist, *Physics,* **32,** 110–113 (1928, rev. ed.).

60. J. B. Johnson, Physics **32,** 97–110 (1928, rev. ed.)

61. H. Brixy, R. Hecker, K. F. Rittinghaus, and H. Howener, ''Applications of Noise Thermometry in Industry under Plant Conditions,'' in *Temperature, Its Measurement and Control in Science and Industry,* J. F. Schooley (ed.), Reinhold, New York, 1982, pp. 1225–1237.

62. H. Brixy, R. Hecker, J. Oehmen, and E. Zimmermann, ''Temperature Measurements in the High-Temperature Range (1000–2000C) by Means of Noise Thermometry,'' *High temperatures–High Pressures* **23**(6) 625–631 (1991).

Copyright © 2006 John Wiley & Sons Retrieved from: www.knovel.com

63. H. A. Tasman and J. Richter, "Unconventional Methods of Temperature Measurement," *High Temperatures—High Pressure* **11,** 87–101 (1974).

64. A. Benjaminson and F. Rowland, *Temperature, Its Measurement and Control in Science and Industry,* Vol. 4, Instrument Society of America, Pittsburgh, PA, 1972, p. 701.

65. J. F. W. Bell, A. A. Fathamani, and T. N. Seth, 1975, cited in Von der Hardt et al., vol. 2, 1975, pp. 649–680.

66. *The Temperature Measurement Handbook and Encyclopedia,* Omega Engineering, Stamford, CT, 1985, p. Q4.

67. R. J. Moffat, "Introduction to Flow Rate Measurement," in *Experimental Methods in the Thermosciences,* Mechanical Engineering Department, Stanford University, Stanford, CA, 1978.

68. H. S. Bean, *Fluid Meters—Their Theory and Application,* 6th ed., (American Society of Mechanical Engineers, New York, 1971).

69. R. P. Benedict, Fundamentals of Temperature, Pressure, and Flow Measurement, 2nd ed., Wiley, New York, 1977.

70. Ultrasonic Doppler and time-of-flight flowmeters, www.enginering toolbox.com

71. J. Flood, "Ultrasonic Flowmeter Basics," *Sensors Magazine,* October 1997.

72. G. Yamanaka, H. Kikura, and M. Aritomi, "Study on Velocity Profile Measurement Using Ultrasound Time-Domain Correlation Method," *ASME HTD* **369**(3), 259–264 (2001).

73. L. Lynnworth, "Clamp-On Flowmeters for Fluids," *Sensors,* August 2001.

74. J. Yoder, "Flowmeters and Their Apps: An Overview," *Sensor Technology and Design,* October 2003.

75. Omega.com, technical reference section: ultrasonic flowmeters.

76. http://www.efunda.com/DesignStandards/sensors/flowmeters/flowmeter_ustt.cfm.

77. C. Ruppel and F. Peters, "Effects of Upstream Installations on the Reading of an Ultrasonic Flowmeter," *Flow Measurement and Instrumentation* **15**(3), 167–177 (June 2004).

78. P. I. Moore, G. J. Brown, and B. P. Stimson, "Ultrasonic Transit-Time Flowmeters Modeled with Theoretical Velocity Profiles: Methodology," *Measurement Science and Technology,* **11,** pp. 1802–1811 (2000).

79. T. T. Yeh, P. I. Espina, and S. A. Osella, "An Intelligent Ultrasonic Flow Meter for Improved Flow Measurement and Flow Calibration Facility," in *Conference Record—IEEE Instrumentation and Measurement Technology Conference,* Vol. 3, 2001, pp. 1741–1746.

80. M. Willatzen, "Ultrasonic Flowmeters: Temperature Gradients and Transducer Geometry Effects," *Ultrasonics* **41,** 105–114 (2003).

81. J. Berrebi, P.-E. Martinsson, M. Willatzen, and J. Delsing, "Ultrasonic Flow Metering Errors Due to Pulsating Flow," *Flow Measurement and Instrumentation* **15**(3), 179–185 (June 2004).

82. C. Carlander, and J. Delsing, "Installation Effects on an Ultrasonic Flow Meter with Implications for Self Diagnosis," *Flow Measurement and Instrumentation* **11**(2), 109–122 (2000).

83. M. J. Vermeulen, G. De Boer, and J. Bowen, "A Model for Estimation of the Ultrasonic Noise Level Emitted by Pressure Regulating Valves and Its Influence on Ultrasonic Flowmeters," in *Proceedings of the Annual ACM-SIAM Symposium on Discrete Algorithms,* 2001, pp. 435–444.

84. I. Fyrippi, I. Owen, and M. P. Escudier, "Flowmetering of Non-Newtonian Liquids," *Flow Measurement and Instrumentation* **15**(3), 131–138 (June 2004).

85. F. J. Weber, H. Johari, and W. W. Durgin, "Ultrasonic Beam Propagation in Turbulent Flow," in *Proceedings of the ASME Fluids Engineering Division Summer Meeting,* Vol. 1, 2003, pp. 85–91.

86. J. Lansing, "Dirty vs Clean Ultrasonic Gas Flow Meter Performance," in *Proceedings of the Annual ACM-SIAM Symposium on Discrete Algorithms,* 2002, pp. 989–999.

Copyrighted Material

Copyright © 2006 John Wiley & Sons Retrieved from: www.knovel.com